Aalto University

OPEN ACCESS

This is an electronic reprint of the original article.
This reprint may differ from the original in pagination and typographic detail.

Hua, Pengmin; Wang, Haichao; Xie, Zichan; Lahdelma, Risto

**Integrated demand response method for heating multiple rooms based on fuzzy logic considering dynamic price**

*Published in:*
Energy

*DOI:*
10.1016/j.energy.2024.132577

Published: 30/10/2024

*Document Version*
Publisher's PDF, also known as Version of record

*Published under the following license:*
CC BY

*Please cite the original version:*
Hua, P., Wang, H., Xie, Z., & Lahdelma, R. (2024). Integrated demand response method for heating multiple rooms based on fuzzy logic considering dynamic price. *Energy*, *307*, Article 132577.
https://doi.org/10.1016/j.energy.2024.132577

This material is protected by copyright and other intellectual property rights, and duplication or sale of all or part of any of the repository collections is not permitted, except that material may be duplicated by you for your research use or educational purposes in electronic or print form. You must obtain permission for any other use. Electronic or print copies may not be offered, whether for sale or otherwise to anyone who is not an authorised user.

Energy 307 (2024) 132577

Contents lists available at ScienceDirect

Energy

journal homepage: www.elsevier.com/locate/energy

# Integrated demand response method for heating multiple rooms based on fuzzy logic considering dynamic price

Pengmin Hua [a,*], Haichao Wang [a,c,**], Zichan Xie [a], Risto Lahdelma [a,b]

[a] Department of Mathematics and Systems Analysis, Aalto University, School of Science, P.O. BOX 11100, Espoo, Finland
[b] Department of Mechanical Engineering, Aalto University, P.O. BOX 14100, FI-00076, Espoo, Finland
[c] School of Infrastructure Engineering, Dalian University of Technology, Dalian, 116024, China

ARTICLE INFO

Handling editor: X Zhao

*Keywords:*
Demand response
District heating
Air source heat pump
Multi-objective model predictive control
Fuzzy logic

ABSTRACT

We consider an educational building heated by a combination of district heating (DH) and a local air source heat pump. We have developed an integrated demand response method for multiple rooms, consisting of an optimization layer and a control layer, to maintain thermal comfort and save energy and costs. For the optimization layer, we apply fuzzy logic to adjust indoor temperature setpoints to respond to dynamic heat prices and propose an optimal heat supply method to find optimal heat supply schemes. For the control layer, a multi-objective model predictive control (MPC) has been developed to manage indoor thermal conditions across multiple rooms. To test and verify the integrated demand response method, we build a multi-room simulation model using the CARNOT Toolbox. The results show that adopting different indoor temperature setpoints during working and nonworking hours, combined with the MPC method, has an energy-saving potential of 9.1 % compared to maintaining a constant indoor temperature using DH alone. Adjusting temperature setpoints using fuzzy logic utilizes the building's heat storage capacity to increase energy flexibility, reaching 16.0 % savings in energy and reducing 12.6 % heating costs.

Nomenclature

| | |
|---|---|
| Abbreviation | |
| EU | European Union |
| DSM | Demand-side management |
| DH | District heating |
| DR | Demand response |
| ASHP | Air source heat pump |
| COP | Coefficient of performance |
| HVAC | Heating, ventilation, and air conditioning |
| MPC | Model predictive control |
| PID | Proportional-integral-derivative |
| CARNOT | **C**onventional **A**nd **R**enewable e**N**ergy systems **O**p**T**imization Blockset |
| RMSE | Root mean squared error |
| NB; NS; ZE; PS; PB | Fuzzy subsets: Negative Big; Negative Small; Zero; Positive Small; Positive Big |
| Symbols | |
| $J$ | Cost function |
| $Q$ | Heat demand/load/consumption, W/kW/MWh |

(*continued on next column*)

(*continued*)

| | |
|---|---|
| $V$ | The volume of room, $m^3$ |
| $T$ | Air temperature, °C |
| $A$ | State transition matrix |
| $B$ | Input matrix |
| $C$ | Output matrix |
| $E$ | Disturbance matrix; Fuzzy inputs of the system |
| $P$ | Control accuracy, percentage, % |
| $\Delta E$ | Fuzzy deviation of deviation between dynamic and average heat prices, (€/MWh) |
| $U$ | Fuzzy output of the system |
| $t$ | time period |
| $\rho$ | Density, kg/$m^3$ |
| $c$ | Heat price, (€/MWh); Specific heat capacity, J/(kg•°C) |
| $x$ | Supplied heat, W; State space vector |
| $y$ | Output vector |
| $u$ | Input vector of state space representation; Real output of system |
| $\Delta u$ | The change rate of the controlled variables |
| $d$ | Disturbance vector |
| $\Delta d$ | The change rate of the disturbance vector |

(*continued on next page*)

* Corresponding author.
** Corresponding author. Department of Mathematics and Systems Analysis, Aalto University, School of Science, P.O. BOX 11100, Espoo, Finland.
*E-mail addresses:* pengmin.hua@aalto.fi (P. Hua), wanghaichao2002@163.com, haichao.wang@aalto.fi (H. Wang), xiezichan@outlook.com (Z. Xie), risto.lahdelma@aalto.fi (R. Lahdelma).

https://doi.org/10.1016/j.energy.2024.132577
Received 13 April 2024; Received in revised form 12 July 2024; Accepted 23 July 2024
Available online 24 July 2024
0360-5442/© 2024 The Authors. Published by Elsevier Ltd. This is an open access article under the CC BY license (http://creativecommons.org/licenses/by/4.0/).

(continued)

| | |
|---|---|
| $h$ | The correction rate |
| $Np$; $Nc$; $N_{in}$ | Discrete prediction horizon; Discrete control horizon; The number of rooms |
| $\tau$ | Continuous time moment |
| $k$ | Discrete time moment |
| $e$ | Error, °C; Real deviation between dynamic and average heat prices, (€/MWh) |
| $\Delta e$ | Real deviation of heat prices between current and next moments, (€/MWh) |
| $\mu$ | Membership function |
| $q,r,w$ | Weights for components of cost function |
| Super/Subscript | |
| $t$ | Time step |
| $d$ | discrete |
| $in$ | indoor |
| $out$ | outdoor |
| $adj$ | adjacent |
| $min$ | minimum |
| $max$ | maximum |
| $rad$ | radiator |
| $mass$ | indoor components (people, lights, equipment) |
| $ven$ | ventilation |
| $win$ | window |
| $gro/flo$ | ground/floor |
| $roof/cei$ | roof/ceiling |
| $cor$ | correction |
| $set$ | setpoints |
| $p/Np$ | prediction horizon (continuous/discrete) |
| $c/Nc$ | control horizon (continuous/discrete) |
| $i, j$ | index |

## 1. Introduction

### 1.1. Background

Buildings consume a share percentage of energy, for example, one-third world-wide and 40 % in the European Union (EU) [1,2]. Across most EU countries, the annual heat demand in buildings exceeds that of electricity and cooling demands [3]. Energy saving in building heating is urgent considering the need of global energy conservation and emission reduction. Demand-side management (DSM) [4] has found success in the power systems of buildings [5], and many scholars have dedicated themselves to using DSM in building heating systems [6–8]. Several main strategies of DSM can be implemented in buildings to increase the flexibility of district heating (DH), such as demand response (DR), which relies on consumers' behavior during peak hours to reduce energy use [9].

### 1.2. Related research and research gaps

The aim of applying DSM in DH is to modify the portion of the building's thermal demand (for space heating and/or domestic hot water) that is supplied by DH to change the overall DH network thermal load. This allows for changing the characteristics of the overall load profile to make it compliant with the production side (i.e., combined heat and power plants, heat-only boilers, geothermal and solar plants, heat recovery systems) [10].

Heating load forecasting, dynamic heat prices, and optimization methods or control strategies are the three main parts of applying DSM to a building's heating systems for flexible energy usage. Regarding heating load forecasting, our previous study has provided a clear description of load forecasting technologies for buildings and districts/cities [11].

Dynamic heat price is closely related to the type of heating source. DH is a typical way to supply heat to buildings and is widely used in many countries. A significant challenge for applying DR to the buildings connected to DH is that the DH price is fixed, and the determination of the DH price is confidential and not open to customers [12]. The customers will not participate in the DSM on the building side without incentives. Due to this reason, more and more researchers suggest using dynamic DH prices and developing some models to calculate the dynamic DH prices [13–15]. Energy companies also try to use some simple dynamic heat pricing schemes. For example, Helen Company in Finland [16] introduces seasonal dynamic DH prices, which correspondingly adopt four different DH prices for four seasons in a year. Typically, the DH price in winter tends to be high, considering the high cost of generating space heating and domestic hot water in cold weather. Fortum Company determines the DH prices based on the outdoor temperatures in the Stockholm area of Sweden [12,17]. Typically, the lower the outdoor temperature, the higher the DH prices. In addition, the DH price is also tied to the maximum heat demand of the building [12]. Thus, the customer can reduce their DH costs both by reducing overall DH consumption and by lower their peak demand. Although the dynamic DH pricing model and calculation methods need to be improved, current attempts have also allowed customers to participate in DSM.

With the development of dynamic electricity prices and the diversity of heating systems on the building side [18], many systems that use electricity to heat buildings have become more popular, such as heat pumps [19]. Air source heat pump (ASHP) is a popular way used in buildings due to its advantages of low operational cost, energy saving, and flexible energy usage. ASHP utilizes electricity to transfer heat from outdoor air to heat the indoor air of the building. The cost of heat generated by ASHP has a tight relationship with the electricity prices, increasing the flexible usage of energy for buildings [20]. In addition, the performance of ASHP also affects the cost of producing heat by ASHP. For example, ASHP has low efficiency in the summer and is prone to frosting in the winter [21,22]. The coefficient of performance (COP) is a crucial factor that characterizes the performance of an ASHP. It is influenced by various factors, including outdoor temperatures, humidity levels, and the capacity of the ASHP [23,24]. The bigger the COP, the higher the efficiency of ASHP. ASHP is no longer a sustainable option when the COP is low enough.

Optimization methods or control strategies for applying DR on the building side have been studied. The realization of DR control is based on efficient control methods, broadly divided into direct and indirect control methods. Among these, price-based control and incentive-based control are the two main indirect control methods, and most studies focus on them. Many control technologies can support the realization of DR control, such as proportional-integral-derivative control (PID) [25,26], rule-based control, fuzzy control [27], optimal control [28], machine learning, deep learning methods [29], and combinations of these control algorithms [30,31]. A summary of control methods in DR can be found in Ref. [44]. The building has significant heating flexibility due to its thermal mass [32]. A good way to cut the heating peaks and the shift time of heat usage is to utilize the thermal storage capacity of buildings by adjusting indoor temperature setpoints to respond to the price changes of energy [33]. Thus, this study focuses on literature review on control method on indoor temperature setpoints. For instance, Hu et al. developed multiple models that integrate electricity price signals and smart algorithms to determine optimal indoor air temperature setpoint schedules for air conditioners. These models aim to achieve the desired trade-offs among electricity costs, thermal comfort, and peak power reductions [34,35]. Salo et al. proposed a control method based on the weather parameters and price signals to adjust the setpoint of electronic thermostat valves in multiple rooms in a building connected to DH [36]. Foteinaki et al. utilized heat load and dynamic heat production cost as signals to control an apartment building's heating system to shift heat load peaks and reduce cost [33]. Romanchenko et al. researched the flexible operation of DH systems on the building side by allowing indoor air temperature setpoint deviations and applying thermal energy storage [37]. Yuan et al. proposed a rule-based DR algorithm that utilized dynamic DH price to achieve the DR control of temperatures for swimming pools and space air in a swimming hall in Finland [38]. Du et al. established a multi-regional dynamic setpoint temperature model to adjust temperature setpoints in different regions dynamically based on demand levels. They applied this method in conjunction with other optimization techniques to the heating, ventilation, and air conditioning (HVAC) system of a building, demonstrating a reduction in load demand by 6.16 % [39]. Xiong et al. proposed an enhanced transactive control method that integrates the real-time electricity price and the user's bidding electricity price to determine temperature setpoints for air-conditioning systems [40]. Li et al. proposed a DR strategy based on reinforcement learning-based temperature setpoint control and active energy storage for an HVAC system to improve energy saving and decrease peak operation [41]. Li et al. proposed a method based on heat balance equations combined with a thermal comfort model to dynamically adjust room temperature setpoints, aiming to tap the energy-saving potential of air-conditioning systems [42].

Previous work has proven that the DR control for indoor air temperature setpoints can cut demand peaks and shift load, increasing flexibility of heat usage and saving cost. However, some aspects require further investigation.

(1) Most previous work focuses on HVAC systems based on dynamic electricity prices, such as [34,35,38–42], and few works focus on the buildings connected to DH. The main reason is that the dynamic pricing of DH is currently not widely applied. Considering the global energy crisis and environmental problems, applying dynamic heat prices, and encouraging customers to participate in the DSM is a future trend.
(2) Previous work on determining indoor temperature setpoints of buildings connected to DH commonly focuses on the building level, such as [33,37]. Considering different spaces in a building have requirement for thermal comfort and therefore different heat demand, it is necessary to apply DR control on the room level in a building.
(3) Previous work's dynamic indoor temperature setpoints method is mainly a rule-based control method, such as [33,36–38]. Normally, a single rule was adopted in previous research. More smart methods need to be applied to determine suitable indoor temperature setpoints to increase the flexible usage of heat for buildings.
(4) ASHP is a typical system used to generate heat for buildings using electricity. The cost of ASHP for generating heat is dynamic because of the dynamic electricity prices and the performance of ASHP. Thus, optimal heat supply schemes need to be further studied when ASHP and DH heat the buildings at the same time. The combination of DH and ASHP also allows studying DR of a district-heated building with currently constant DH price.

### 1.3. Research gaps and novelty

This study aims to address the identified gaps, and therefore, the research novelties are as follows:

(1) We have developed a novel integrated DR method for multiple rooms with different requirements for thermal comfort, consisting of an optimization layer and a control layer to maintain thermal comfort and save energy and costs.
(2) The control layer applies a novel multi-objective predictive control (MPC) with a simple physical room model, and multi-objective optimization is proposed to control the indoor temperature for multiple rooms with different thermal comfort requirements with reasonable control accuracy in a building.
(3) Our work is the first attempt to apply fuzzy logic to adjust the dynamic indoor temperature setpoints based on the dynamic heat prices with various heat sources to increase the flexibility of energy usage.
(4) An optimal heat supply scheme with minimum operation cost has been found considering many factors, such as the performance of ASHP, etc., to supply heat to the rooms in a building heated by ASHP and DH.

The remainder of this paper is organized as follows: Section 2 introduces the case study and the model of rooms incorporated into the **C**onventional **A**nd **R**enewable e**N**ergy systems **O**p**T**imization Blockset (CARNOT Toolbox). Section 3 introduces a methodology that contains optimization and control layers and evaluation indicators. Section 4 presents the simulation schemes and application scenarios. Section 5 analyzes the results of all scenarios. Finally, Section 6 concludes the paper.

## 2. CARNOT model development for multiple heating rooms

This section presents the details of the multiple rooms studied in this case and the CARNOT model constructed to simulate indoor temperatures.

### 2.1. Case introduction

The case model is developed for multiple rooms on the top floor of an educational building in Espoo, Finland. The rooms are used for teaching, teamwork, and self-study. The floor plan of target rooms is shown in Fig. 1.

There are three kinds of spaces in the building. Rooms 1 to 3 face an exterior wall with windows, and their indoor temperature is susceptible to weather and may change rapidly. Rooms 4 and 5 are rooms without exterior walls, and their indoor temperature varies more smoothly. Usually, their indoor temperature can be maintained in a suitable range with very little heating compared to the first kind of space. The third kind of space is corridors where people only stay for a short period. The corridor is divided into Room 6 and Room 7 because Room 6 has an exterior wall, while Room 7 does not. To save energy, the temperature setpoints of corridors can be a little lower than that for office rooms. These three kinds of spaces are typical for many buildings. Considering them in our study aims to make our research results more universal and applicable to other cases. The details of these rooms are shown in Table 1.

### 2.2. Multiple rooms model in CARNOT toolbox

Fig. 2 shows the CARNOT model for the multiple rooms. The top part in Fig. 2 shows the whole multiple rooms model. To make it clear, we only show the inputs and outputs of this model. The inputs include weather parameters, supply water temperature, and water flow for the radiators in each room. The outputs are the simulated indoor temperature of each room. The middle part of Fig. 2 provides more details of this multiple rooms model. It contains seven single-room models and interactions between different single-room models, illustrated by connecting lines. The details of Simulink modules of all rooms are shown in Appendix A. In addition to the inputs shown in the top part, the inputs also include inner heat gain of indoor components, mainly heat gain of people, lights, and equipment. The inner heat gains of indoor components vary across different rooms. Take Room 1 for an example, the bottom part of Fig. 2 illustrates the model structure for Room 1. Each room model contains various components, such as walls, windows, floor, ceiling, and radiator. Parameters, such as density, thickness, heat capacity, and heat transfer coefficient, are defined in the component models.

To verify the accuracy of the multiple rooms model in the CARNOT Toolbox, we conducted several experiments in the actual rooms. First, we switched off the radiators of target rooms for two weeks, from 5th to December 18, 2022, and recorded the indoor temperatures. During this period, the target rooms' temperature is mainly affected by weather parameters and heat exchange between different rooms. The measured indoor temperatures during these two weeks are used to verify the

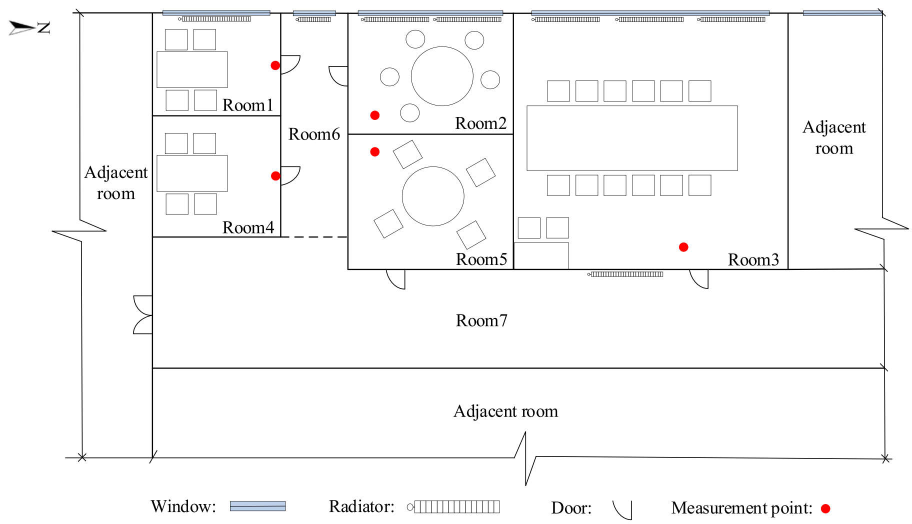


**Fig. 1.** The plan of multiple rooms.

**Table 1**
Properties and parameters of target multiple rooms.

| Room number | Structure name of room: Number/Parameters (area (m$^2$)/heat transfer coefficient (W/(m$^2$·K)) or power (W)) | | | | | |
|---|---|---|---|---|---|---|
| | Exterior walls | Interior walls | Roofs | Floors | Internal heat gains | Radiators |
| 1 | Wall:1/4.11/0.18<br>Window: 1/4.44/0.94 | 1/8.12/1.49<br>1/8.12/2.97<br>1/8.55/1.50 | 1/8.55/0.09 | 1/8.55/1.49 | Maximum occupancy: 4<br>Light: 2/28<br>Screen: 1/220 | 1 |
| 2 | Wall:1/7.02/0.18<br>Window: 1/6.66/0.94 | 1/11.54/2.97<br>1/11.54/1.49<br>1/13.68/1.50 | 1/19.44/0.09 | 1/19.44/1.49 | Maximum occupancy: 6<br>Light: 5/28<br>Screen: 1/220 | 2 |
| 3 | Wall:1/11.48/0.18<br>Window: 1/9.90/0.94 | 1/20.95/1.49<br>1/20.95/1.49<br>1/21.38/1.49 | 1/55.13/0.09 | 1/55.13/1.49 | Maximum occupancy: 20<br>Light: 9/28<br>Screen: 1/220 | 3 |
| 4 | – | 1/6.84/1.49<br>1/6.84/2.97<br>1/10.26/1.05 | 1/8.64/0.09 | 1/8.64/1.49 | Maximum occupancy: 4<br>Light: 2/28<br>Screen: 1/220 | – |
| 5 | – | 1/9.41/1.05<br>1/9.41/1.49<br>1/13.68/2.97 | 1/15.84/0.09 | 1/15.84/1.49 | Maximum occupancy: 6<br>Light: 6/28<br>Screen: 1/220 | – |
| 6 | Wall:1/2.64/0.18<br>Window: 1/2.06/0.94 | 1/16.67/2.97<br>1/20.95/2.97 | 1/12.13/0.09 | 1/12.13/1.49 | Light: 4/28 | 1 |
| 7 | – | 1/4.95/1.49<br>1/50.02/1.49<br>1/50.02/1.49 | 1/36.31/0.09 | 1/36.31/1.49 | Light: 11/28 | 1 |

accuracy of the CARNOT Toolbox in modeling the structures of target rooms and adjacent rooms. Then we turned on the radiators of target rooms during the following two weeks, from December 19, 2022 to January 1, 2023, and recorded the indoor temperatures. During this period, in addition to weather parameters and heat exchange between different rooms, the target rooms' temperature is mainly affected by heat provided by radiators. The measured indoor temperature during these two weeks is used to verify the accuracy of the CARNOT Toolbox in modeling heating systems in target rooms.

The measured and simulated indoor temperatures of target rooms for four weeks in winter are shown in Fig. 3. Both during non-heating and heating periods, the simulated temperatures can cover the measured temperatures well and the root mean squared error (RMSE) for Rooms 1 to 5 is 0.52, 0.36, 0.30, 0.29, and 0.39 °C, respectively, indicating that the CARNOT model accurately simulates the room temperature.

In addition, based on the measured data, the indoor temperatures of all rooms tend to be lower than 20 °C during the non-heating period, especially for the rooms that have exterior walls and windows. The indoor temperatures of all rooms can be maintained within a reasonable range, 20 °C–24 °C, during the heating period. The indoor temperatures during nonworking hours tend to be higher than anticipated, which leads to a waste of energy because the rooms are mostly empty during nonworking hours, e.g., on weekends. Thus, an optimal control strategy for indoor temperatures is necessary.

## 3. Methodology

This section introduces the integrated DR method for the heating system of the building, shown in Fig. 4. This integrated DR method contains an optimization layer and a control layer. The optimization layer optimizes the hourly heat acquisition and applies fuzzy logic for DR. Heat acquisition costs are minimized considering different available heat sources and dynamic price. Fuzzy logic is used adjust indoor temperature setpoints considering the thermal storage capacity of the building and changes in energy price, aiming to reduce heating peaks and shift the time of heat usage. The indoor temperature setpoints are inputs to the MPC method in the control layer. In the control layer, the multi-objective MPC method is adapted to find the optimal supply water flow for each room and calculate the total heat demand of the system. The calculated optimal supply water flows are inputs to the multiple

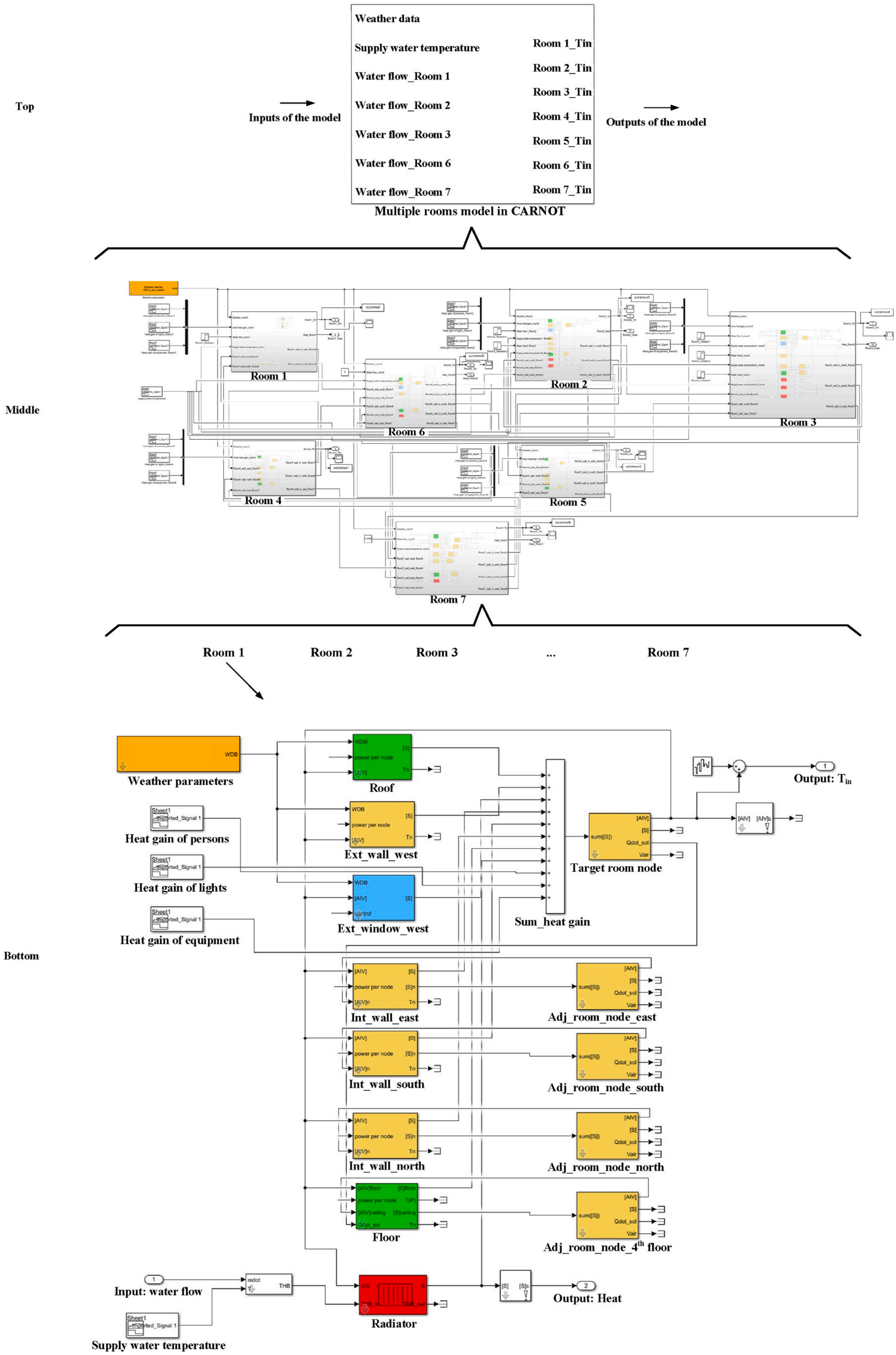


**Fig. 2.** Multiple rooms model in CARNOT Toolbox.

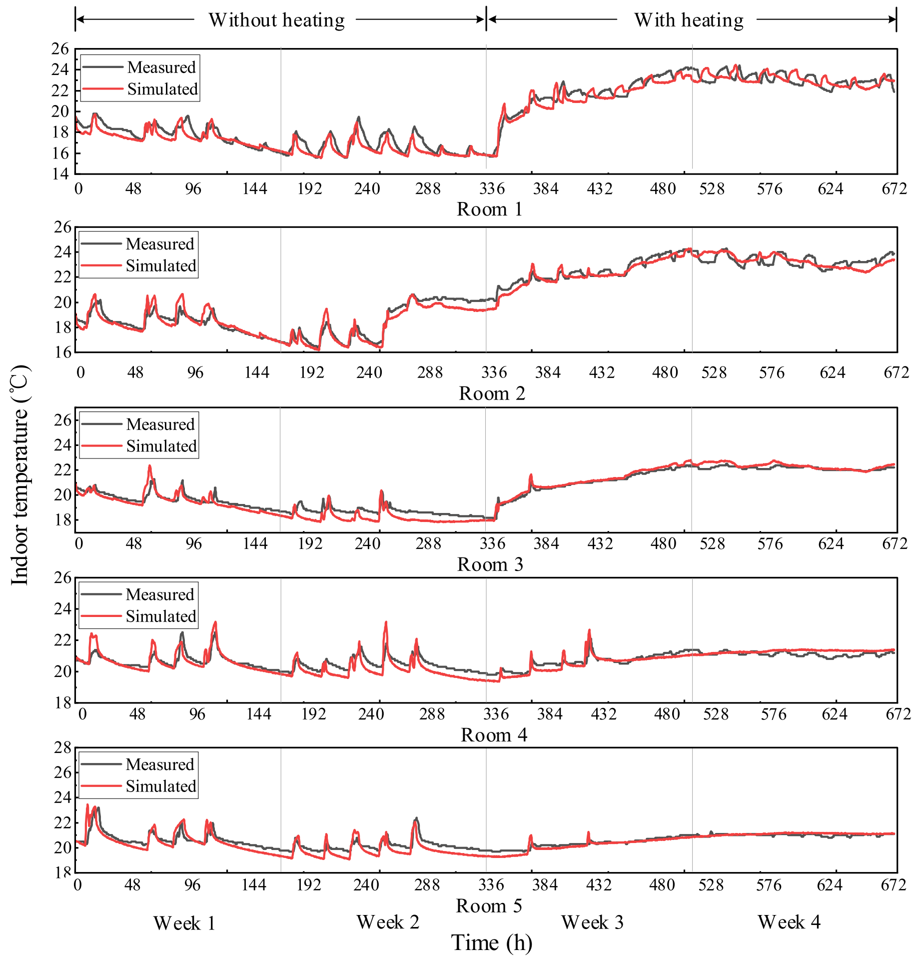


**Fig. 3.** Measured and simulated indoor temperatures of rooms from December 5, 2022 to January 1, 2023.

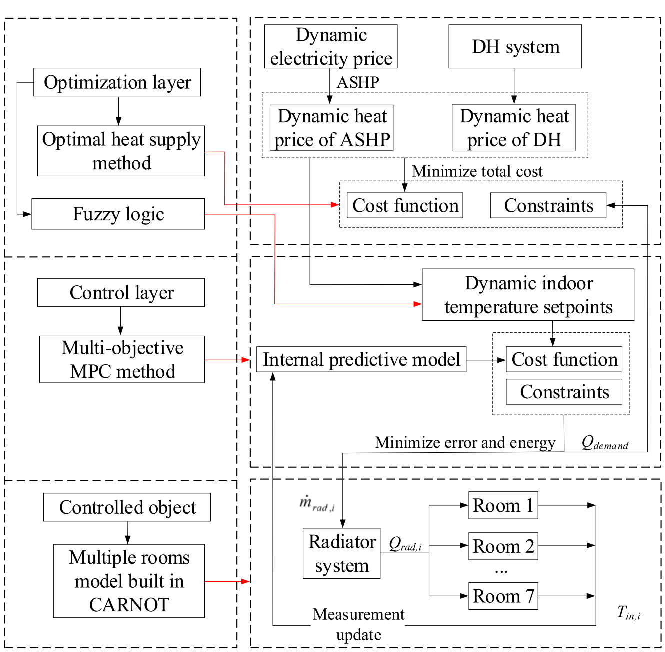


**Fig. 4.** Algorithm framework.

rooms model and the calculated total heat demand is the input for the optimal heat supply method.

### 3.1. *Optimization layer*

The optimization layer contains the optimal heat supply method and fuzzy logic to choose an optimal heat supply scheme and adjust dynamic indoor temperature setpoints based on dynamic heat prices.

#### 3.1.1. *Optimal heat supply method*

We assume that DH and ASHP can provide heat for the building separately or together. Minimizing the heating costs in each time step can be formulated as a linear optimization model in Equations (1a) & (1b). More complicated heating systems can be defined easily.

$$J_t = \min\left(c_t^{ASHP} x_t^{ASHP} + c_t^{DH} x_t^{DH}\right) \tag{1a}$$

$$\text{Subject to}: \begin{cases} 0 \leq x_t^{ASHP} \leq x_{capacity}^{ASHP} \\ 0 \leq x_t^{DH} \leq x_{capacity}^{DH} \\ x_t^{ASHP} + x_t^{DH} = Q_t^{demand} \end{cases} \tag{1b}$$

Here, $c_t^{ASHP}$ and $c_t^{DH}$ (€/MWh) are heat price of ASHP and DH, $x_t^{ASHP}$ and $x_t^{DH}$ (MWh) are heat supplied by ASHP and DH, and $Q_t^{demand}$ (MWh) is the combined heat demand of all rooms at time step *t*. $x_{capacity}^{ASHP}$ and $x_{capacity}^{DH}$ (MWh) are the maximum capacity of ASHP and DH. The optimal solution is to use primarily the cheaper energy source and supplement that with the more expensive source only when demand exceeds the capacity of the cheaper source. The marginal price of heat is the price of the most expensive heat source used at time step $t$.

### 3.1.2. Fuzzy logic for dynamic indoor temperature setpoints

In real projects, it is difficult to find a crisp mathematics model for them when the relationship between two variables is complex. Fuzzy logic offers several advantages, particularly in systems and applications where precision and certainty are challenging to achieve. For example, fuzzy logic is adept at managing uncertainty and imprecise information, making it useful in real-world scenarios where data might be incomplete, noisy, or vague. Fuzzy logic allows the use of linguistic variables (e.g., "high," "medium," "low" instead of numerical ones, making system design more intuitive and closer to human reasoning.

In our case, based on the experts' experience, we want the indoor temperature setpoints can be a little higher when the heat price is low to store more heat in the building mass and lower when the heat price is high. However, "higher" and "lower" are two fuzzy concepts, and it is hard to describe them using precise models. Fuzzy logic can express an expert's experience in fuzzy rules, suitable for adjusting indoor temperature setpoints based on dynamic heat prices. It involves three steps:

Fuzzifications: Exact (crisp) inputs are converted into fuzzy inputs.

Reasoning process: Fuzzy "IF-THEN" type rules are applied to the fuzzy inputs to reach fuzzy outputs.

Defuzzification: The fuzzy outputs are converted into crisp outputs.

Here, we apply Mamdani-type fuzzy "min-max" rules, where the firing strength of each rule is determined by taking the minimum of the membership values associated with the inputs, and rules are aggregated by the maximum of their individual firing strength [43].

## 3.2. Control layer

In previous research [44], we introduced a multi-objective MPC method coupled with a straightforward internal predictive model for a single room, demonstrating its applicability. In this study, we extended the application of this method to the indoor thermal comfort control of multiple rooms.

### 3.2.1. Internal predictive model and state space representation for multiple rooms

The physical model for a single room is constructed based on the principles of energy conservation, as shown below.

$$\rho_{in} c_{in} V_{in} \frac{dT_{in}}{d\tau} = Q_{rad} + Q_{mass} + Q_{solar} + Q_{ven} - Q_{win} - Q_{gro/flo} - Q_{roof/cei} - Q_{wall} \tag{2}$$

Here, $Q_{rad}$, $Q_{mass}$, $Q_{solar}$, and $Q_{ven}$ represent the heat gained from radiators, indoor components (people, lights, and equipment), solar radiation through windows, and heat provided by the ventilation system, W. Additionally, $Q_{win}$, $Q_{gro.flo}$, $Q_{roof/cei}$, and $Q_{wall}$ represent heat exchange through windows, ground/floor, roof/ceiling, and walls (including interior and exterior walls), W. The proposed internal predictive model can meet the MPC control requirements. For details on the calculation of each term in equation (2) and analysis of the proposed internal predictive model, refer to our previous research [44]. We rewrite the multiple rooms model into the state space representation and discretize it, as shown in (3).

$$\begin{aligned} x(k+1) &= A_d x(k) + B_d u(k) + E_d d(k) \\ y(k+1) &= C_d x(k+1) \end{aligned} \tag{3}$$

$x$ is the state space vector representing the multiple rooms' indoor temperatures. $y$, $u$, and $d$ are the output, control, and disturbance vectors. $A_d$, $B_d$, $C_d$, and $E_d$ are the state transition matrix, the input matrix, the output matrix, and the matrix describing disturbances, respectively. The current moment is denoted by $k$, and the subsequent moment is denoted by $k$+1. The predicted indoor temperatures at different moments within the prediction horizon can be expressed as (4). We define equations (5) and (6) to represent $u$ and $d$ in terms of incremental changes $\Delta u$ and $\Delta d$.

$$\begin{aligned} x(k+1|k) &= A_d x(k) + B_d u(k) + E_d d(k) x(k+2|k) = A_d^2 x(k) + A_d B_d u(k) \\ &+ B_d u(k+1|k) + A_d E_d d(k) + E_d d(k+1|k) x(k+3|k) \\ &= A_d^3 x(k) + A_d^2 B_d u(k) + A_d B_d u(k+1|k) + B_d u(k+2|k) \\ &+ A_d^2 E_d d(k) + A_d E_d d(k+1|k) + E_d d(k+2|k) \vdots x(k+N_p|k) \\ &= A_d^{N_p} x(k) + A_d^{N_p-1} B_d u(k) + A_d^{N_p-2} B_d u(k+1|k) \\ &+ \cdots + B_d u(k+N_p-1|k) + A_d^{N_p-1} E_d d(k) + A_d^{N_p-2} E_d d(k+1|k) \\ &+ \cdots + E_d d(k+N_p-1|k) \end{aligned} \tag{4}$$

$$\begin{aligned} u(k) &= \Delta u(k) + u(k-1) \\ u(k+1|k) &= \Delta u(k+1|k) + \Delta u(k) + u(k-1) \\ u(k+2|k) &= \Delta u(k+2|k) + \Delta u(k+1|k) + \Delta u(k) + u(k-1) \\ &\vdots \\ u(k+N_p-1|k) &= \Delta u(k+N_p-1|k) + \cdots + \Delta u(k+1|k) + \Delta u(k) + u(k-1) \end{aligned} \tag{5}$$

$$\begin{aligned} d(k) &= \Delta d(k) + d(k-1) \\ d(k+1|k) &= \Delta d(k+1|k) + \Delta d(k) + d(k-1) \\ d(k+2|k) &= \Delta d(k+2|k) + \Delta d(k+1|k) + \Delta d(k) + d(k-1) \\ &\vdots \\ d(k+N_p-1|k) &= \Delta d(k+N_p-1|k) + \cdots + \Delta d(k+1|k) + \Delta d(k) + d(k-1) \end{aligned} \tag{6}$$

We acquire the predicted indoor temperatures of multiple rooms for the prediction horizon, as shown in (7). The complete expression of (7) is shown in Appendix B.

$$\begin{aligned} Y(k) = \Omega X(k) &= \Omega \Phi x(k) + \Omega G_y \Delta U(k) + \Omega \Gamma u(k-1) + \Omega N \Delta D(k) \\ &+ \Omega M d(k-1) \end{aligned} \tag{7}$$

### 3.2.2. Receding horizon optimization

We define the cost function as the weighted sum of three components [44]: tracking error between corrected predictive and indoor temperature setpoints, the change rate of controlled variables, and the energy use for the system, as shown in (8).

$$\begin{aligned} J = min\Bigg( \sum_{j=1}^{N_p} \sum_{i=1}^{N_{in}} q_{ij} \Big( \big( y_{cor,i}(k+j|k) - y_{set,i}(k+j|k) \big) \Big)^2 + \sum_{j=1}^{N_c} \\ \times \sum_{i=1}^{N_{in}} r_{ij} \Delta u_i(k+j|k)^2 + \sum_{j=1}^{N_c} \sum_{i=1}^{N_{in}} w_{ij} u_i(k+j|k) \Bigg) \end{aligned} \tag{8a}$$

$$\text{Subject to:} \quad \begin{aligned} u_{min,i} \le u_i(k+j|k) \le u_{max,i}, \\ \Delta u_{min,i} \le \Delta u_i(k+j|k) \le \Delta u_{max,i}, \\ \Delta u_i(k+j|k) = u_i(k+j|k) - u_i(k+j-1|k), j = 1, \ldots, N_c, i = 1, \ldots, N_{in} \end{aligned} \tag{8b}$$

[$u_{min,i}$, $u_{max,i}$] is the controlled variable for the multiple rooms. [$\Delta u_{min,i}$, $\Delta u_{max,i}$] restricts the change in water flow within a reasonable range to maintain a stable hydraulic system. The parameters $q_{ij}$, $r_{ij}$, and $w_{ij}$ serve as weights for the three components of the objective function. Nin denotes the number of rooms.

### 3.2.3. Feedback and correction

$e(k)$ represents the error between the actual indoor temperature $y(k)$ and the predicted indoor temperature at the last moment, as shown in (9). We utilize a parameter h, ranging between 0 and 1, to adjust how much $e(k)$ corrects the temperature. Instead of using predictive indoor temperature $y(k+j|k)$, we incorporate the corrected predictive indoor temperature $y_{cor}(k+j|k)$, as shown in (10), into the cost function, as shown in (8). Finally, the corrected output of the system is shown in (11).

$$e(k) = y(k) - y(k|k-1) \tag{9}$$

$$y_{cor}(k+j|k) = y(k+j|k) + he(k)\, j = 1, 2, \ldots, N_p \tag{10}$$

$$Y_{cor}(k) = \Omega\Phi x(k) + \Omega G_y \Delta U(k) + \Omega\Gamma u(k-1) + \Omega N \Delta D(k) + \Omega M d(k-1) + HE(k) \tag{11}$$

Here,

$$H = \begin{bmatrix} h & 0 & \cdots & 0 \\ 0 & h & \cdots & 0 \\ \vdots & \vdots & \ddots & \vdots \\ 0 & 0 & \cdots & h \end{bmatrix};\ E(k) = \begin{bmatrix} e(k) \\ e(k) \\ \vdots \\ e(k) \\ e(k) \\ \vdots \\ e(k) \end{bmatrix}.$$

### 3.3. Evaluation indicators

We use three indicators to measure the control accuracy, energy consumption, and cost.

(1) Control accuracy: We regard that the control accuracy is satisfied if the errors between controlled indoor temperatures and setpoints are in the range [-1 °C, 1 °C]. Thus, we define satisfaction percentage, shown in equation (12), to evaluate control accuracy. tsatisfied is the period when the errors are within the range [-1 °C, 1 °C], and ttotal is the total simulation period.

$$P_{satisfied} = \frac{t_{satisfied}}{t_{total}} \cdot 100\% \tag{12}$$

(2) Heat consumption: Simulated supplied heat from radiators in CARNOT Toolbox.
(3) Cost: Calculated total operation cost during the whole simulation period.

## 4. Simulation schemes and application scenarios

This section outlines the application of the methodology in multiple rooms and the schemes that require analysis.

### 4.1. The application of optimal heat supply method

We obtain the dynamic electricity prices in Nord Pool [45] and the simulation period is from 5th to December 18, 2022. The electricity price from Nord Pool is special because it is much higher than that during the same period in a typical year due to energy problems. Thus, we corrected the electricity prices based on the data in typical years. Considering the ASHP is located on the building side, in addition to the electricity prices, we also need to consider transmission fee, retailer margin, and electricity tax, which are 40.67 (€/MWh), 2.98 (€/MWh), 22.53 (€/MWh), respectively, and value added tax rate is 24 % [46]. Finally, we use these corrected electricity prices to calculate the dynamic heat prices of ASHP. ASHP utilizes electricity to generate heat, and the efficiency of the heat pump is determined by the COP factor, which represents the ratio between produced heat and consumed electricity. The COP factor of an ASHP depends on outdoor temperature and we compute the COP factor based on [23]. Then, we combine the corrected dynamic electricity prices and COP to calculate the dynamic heat prices from 5th to December 18, 2022, shown in Fig. 5, marked red. The black line is the DH prices of Helen Company [16] in Finland. The seasonal prices of DH in a short period are fixed. Sometimes, the heat prices of the ASHP are higher than that of DH, while other times, they are the opposite. To minimize the heating cost, at each moment in time the cheaper source of heat is used first, and the more expensive heat source is used as a supplement only when the cheaper source does not have sufficient capacity. In this study, we assume that the capacity of the ASHP does not depend on outdoor temperature. The ASHP capacity is set to 70 % of maximal heating demand, and we consider also 60 % and 80 % dimensioning as sensitivity analysis.

### 4.2. The application of fuzzy logic to determine temperature setpoints

Based on the dynamic heat prices shown in Fig. 5, we calculate the dynamic indoor temperature setpoints using fuzzy logic. The steps are as follows.

Step 1 Normally, we know the hourly dynamic heat prices one day in advance. We first calculate the average heat price.

Step 2 We determine two real inputs and one output, represented as $e_t$, $\Delta e_t$, and ut. Input $e_t$ ($= c_t$ - $c_{average,24}$) is the deviation between the dynamic and the average heat prices at time t. Input $\Delta e_t$ ($= e_t$ - $e_{t+1}$) is how much the current $e_t$ differs from the next time $e_{t+1}$. Output $u_t$ is the dynamic indoor temperature setpoint at moment $t$. We can calculate the real domain of inputs, [$e_{min}$ $e_{max}$] and [$\Delta e_{min}$ $\Delta e_{max}$], when we obtain $e_t$ and $\Delta e_t$. The fuzzy domain of two inputs and one output, [$E_{min}$ $E_{max}$], [$\Delta E_{min}$ $\Delta E_{max}$], and [$U_{min}$ $U_{max}$], is determined as [-2, 2]. Taking $E_t$ as an example, we obtained the fuzzy inputs using equation (13).

$$E_t = \frac{(e_t - e_{\min})(E_{\max} - E_{\min})}{e_{\max} - e_{\min}} + E_{\min} \tag{13}$$

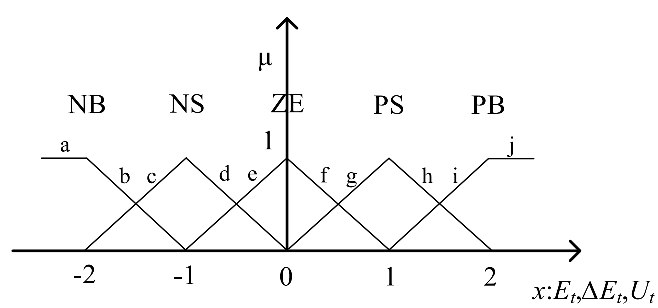


**Fig. 6.** Triangular membership function.

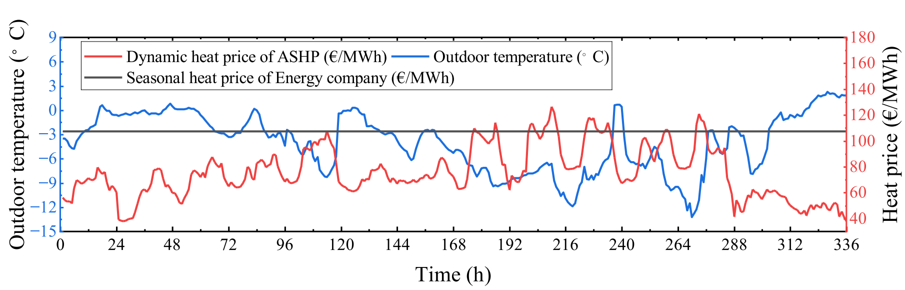


**Fig. 5.** Dynamic heat prices of ASHP and seasonal heat price of energy company from 5th to December 18, 2022.

**Table 2**
Mamdani-type fuzzy rule of dynamic indoor temperature setpoints.

| Et / ΔEt Ut | NB | NS | ZE | PS | PB |
|---|---|---|---|---|---|
| NB | PB | PB | PS | PS | ZE |
| NS | PB | PS | PS | ZE | NS |
| ZE | PS | PS | ZE | NS | NS |
| PS | PS | ZE | NS | NS | NB |
| PB | ZE | NS | NS | NB | NB |

Step 3 Determine the triangular membership function, shown in Fig. 6.

The fuzzy subsets of two fuzzy inputs and one fuzzy output are determined as NB, NS, ZE, PS, and PB, representing Negative Big, Negative Small, Zero, Positive Small, and Positive Big, respectively. We determine Mamdani-type fuzzy rule in Table 2 based on two experiences:

(1) Compare the dynamic heat price with the average heat price. Increase the indoor temperature setpoint when the dynamic heat price is low and decrease the indoor temperature setpoint when the dynamic heat price is high.
(2) Raise the indoor temperature setpoint when the current moment's heat price is lower than that of the next moment to accumulate more heat. Lower the indoor temperature setpoint when the current moment's heat price is higher than that of the next moment to conserve energy.

Then, the fuzzy output $U_t$ can be calculated from the fuzzy inputs, membership function, and Mamdani-type fuzzy rule [43].

Step 4 : Calculate the dynamic room temperature setpoints based on equation (14). This study determines the real domain of output, [umin umax], as [16.5 °C 17.5 °C] during nonworking hours and [20.5 °C 21.5 °C] during working hours.

$$u_t = \frac{(U_t - U_{\min})(u_{\max} - u_{\min})}{U_{\max} - U_{\min}} + u_{\min} \tag{14}$$

### 4.3. Control platform for multiple rooms using MPC in simulink

The internal predictive model for multiple rooms in this study is shown in Appendix. We determine the state space vector $x = [T_{in,1}\ T_{in,2}\ T_{in,3}\ T_{in,4}\ T_{in,5}\ T_{in,6}\ T_{in,7}]^T$, the control vector $u = [Q_{rad,1}\ Q_{rad,2}\ Q_{rad,3}\ Q_{rad,4}\ Q_{rad,5}\ Q_{rad,6}\ Q_{rad,7}]^T$, and the disturbance vector $d = [T_{out}\ I_{solar}\ T_{in,adj1}\ T_{in,adj2}\ T_{in,adj3}\ T_{in,adj4}\ T_{in,adj5}\ T_{in,adj6}]^T$. $T_{in,i}$ represents the indoor temperature of each room, from 1 to 7. $Q_{rad,i}$ represents the supplied heat to each room, from 1 to 7. Tout and $I_{solar}$ are the outdoor temperatures and solar radiation. $T_{in,adj,j}$ are the indoor temperatures of adjacent rooms, from 1 to 6. The discrete state space representation for the multiple rooms is shown in (15).

$$\begin{gathered}
A_d = \begin{bmatrix}
9.98e^{-1} & 0 & 0 & 2.99e^{-4} & 0 & -1.65e^{-3} & 0 \\
0 & 9.98e^{-1} & 2.50e^{-4} & 0 & 2.99e^{-4} & 2.50e^{-4} & 0 \\
0 & 8.83e^{-5} & 1.00 & 0 & 7.20e^{-5} & 0 & 1.64e^{-4} \\
5.04e^{-4} & 0 & 0 & 9.98e^{-1} & 0 & 6.65e^{-4} & 3.53e^{-4} \\
0 & 3.67e^{-4} & 2.50e^{-4} & 0 & 9.98e^{-1} & 1.76e^{-4} & 7.26e^{-4} \\
6.96e^{-4} & 8.17e^{-4} & 0 & 4.84e^{-4} & 2.35e^{-4} & 9.97e^{-1} & 2.69e^{-6} \\
0 & 0 & 2.92e^{-4} & 9.88e^{-5} & 3.73e^{-4} & 1.03e^{-6} & 9.99e^{-1}
\end{bmatrix}; \\
B_d = \mathrm{diag}(\,0.815 \quad 0.613 \quad 0.215 \quad 0 \quad 0 \quad 1.000 \quad 0.385\,); \\
E_d = \begin{bmatrix}
1.44e^{-4} & 2.59e^{-5} & 2.84e^{-4} & 0 & 0 & 0 & 3.59e^{-4} & 0 \\
1.64e^{-4} & 2.91e^{-5} & 0 & 0 & 0 & 0 & 0 & 4.22e^{-4} \\
1.09e^{-4} & 1.53e^{-5} & 0 & 0 & 0 & 1.60e^{-4} & 0 & 4.22e^{-4} \\
2.55e^{-5} & 0 & 3.34e^{-4} & 0 & 0 & 0 & 4.22e^{-4} & 0 \\
2.55e^{-5} & 0 & 0 & 0 & 0 & 0 & 0 & 4.22e^{-4} \\
1.09e^{-4} & 1.47e^{-5} & 0 & 0 & 0 & 0 & 4.31e^{-4} & 0 \\
3.00e^{-5} & 0 & 9.62e^{-5} & 5.72e^{-4} & 1.55e^{-6} & 0 & 0 & 0
\end{bmatrix}
\end{gathered} \tag{15}$$

The MPC platform for the multiple rooms in Simulink is shown in Fig. 7. For the MPC controller, the inputs include dynamic indoor temperature setpoints, calculated based on fuzzy logic, and simulated indoor temperatures from the CARNOT room model. The outputs are water flow for the radiators, which is the optimization results of the controller. The outputs of the MPC controller are also the inputs of the CARNOT room model. For the CARNOT room model, the weather parameters are obtained from a weather station, and the supply water temperature, which correlates linearly with outdoor temperature in Finland, is acquired from the operation scheme. The prediction horizon, control horizon, and control step are set to 90 min, 45 min, and 15 min, respectively. The weights matrix of the cost function, $q_{ij}$, $r_{ij}$, $w_{ij}$ shown in equation (8), are shown as follows. Our previous research [44] introduces how to determine these parameters.

$$q_{ij} = I_7; r_{ij} = 3000 \begin{bmatrix} 1 & \cdots & 1 \\ \vdots & \ddots & \vdots \\ 1 & \cdots & 1 \end{bmatrix}_{3\times 7}; w_{ij} = \begin{bmatrix} 1 & \cdots & 1 \\ \vdots & \ddots & \vdots \\ 1 & \cdots & 1 \end{bmatrix}_{3\times 7}.$$

### 4.4. Scenarios

The simulation period is two weeks, from the 5 to the December 18, 2022. We designed five scenarios with applications of different combinations of proposed optimization methods in this study, as shown in Table 3.

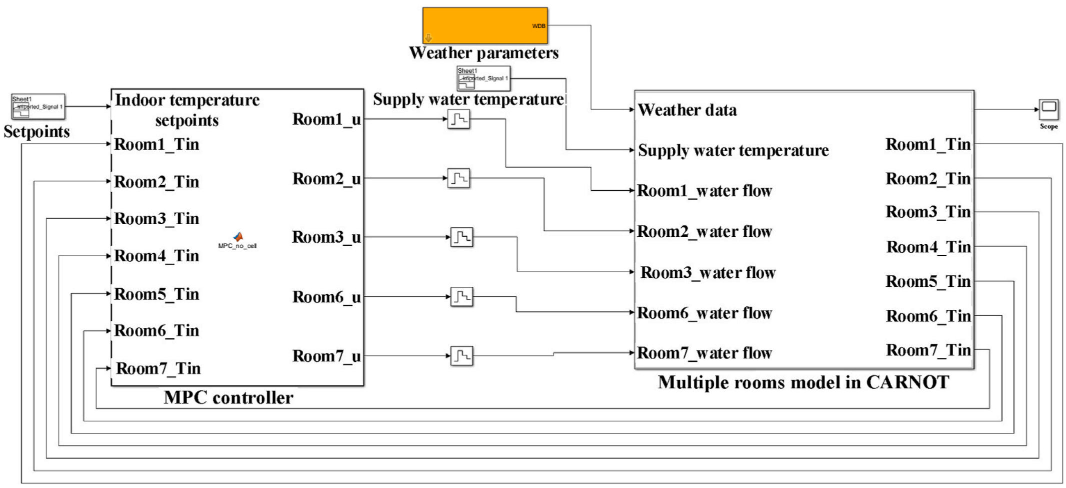


**Fig. 7.** MPC control platform for multiple rooms in Simulink.

**Table 3**
Details of scenarios.

| Scenarios | Multi-objective MPC | Constant heat price of DH | Dynamic heat price of ASHP | Indoor temperature setpoints | | Optimal heat supply |
|---|---|---|---|---|---|---|
| | | | | Fixed | Dynamic | |
| 1 | | ✓ | | | | |
| 2 | ✓ | ✓ | | ✓ | | |
| 3 | ✓ | ✓ | ✓ | ✓ | | |
| 4 | ✓ | ✓ | ✓ | ✓ | | ✓ |
| 5 | ✓ | ✓ | ✓ | | ✓ | ✓ |

**Table 4**
Evaluation indictors of each scenario.

| Scenarios | Psatisfied (%) | Heat consumption (kWh) | Total cost (€) |
|---|---|---|---|
| 1 | – | 212.01 | 22.78 |
| 2 | 91.7 | 192.72 | 20.71 |
| 3 | 91.7 | 192.72 | 16.50 |
| 4 | 91.7 | 192.72 | 16.38 |
| 5 | 88.3 | 161.91 | 14.31 |

(1) Scenario 1: Current operating mode with constant heat price of DH.
(2) Scenario 2: Use constant heat price for DH and apply MPC. Considering that the office rooms are normally empty during nonworking hours, it is possible to lower the temperature setpoints. For special rooms, such as corridors and storage rooms, it is also unnecessary to maintain the temperature setpoint at a high level, such as 21 °C, because people only spend a little time in these rooms. Thus, it is necessary to apply independent indoor thermal control for rooms with different functions in a building. Thus, for office rooms, the temperature setpoints are 21 °C for working hours and 17 °C for nonworking hours. The working hours are set from 7:00 to 21:00 from Monday to Friday, from 9:00 to 14:00 on Saturday, and from 9:00 to 12:00 on Sunday. Regarding the corridor, the temperature setpoint is maintained at 17 °C throughout the day.
(3) Scenario 3: Based on Scenario 2, assume that ASHP is installed and can work together with DH. The COP of ASHP is high enough. Priority should be given to using ASHP for heating, and DH should be used only when ASHP reaches its maximum capacity.
(4) Scenario 4: Based on Scenario 2, assume that ASHP is installed and can work together with DH. The COP of ASHP becomes low when the outdoor temperature is low enough. Use constant heat price for DH and dynamic heat price for ASHP and apply MPC. Optimize the heat supply based on dynamic heat price to minimize the cost in each time step.
(5) Scenario 5: Based on Scenario 4, use fuzzy logic to adjust temperature setpoints based on dynamic heat prices. Depending on the operating situation, that can be the dynamic price of ASHP or the constant price of DH. At the same time, apply the optimal heat supply method.

**Table 5**
Average indoor temperature for multiple rooms.

| Room number | Average indoor temperature (°C) | | | |
|---|---|---|---|---|
| | Scenario 1 | | Scenario 2 | |
| | Working hours | Nonworking hours | Working hours | Nonworking hours |
| 1 | 21.25 | 20.71 | 20.90 | 18.66 |
| 2 | 21.40 | 20.67 | 20.93 | 18.88 |
| 3 | 21.25 | 20.78 | 20.63 | 19.44 |
| 4 | 20.85 | 20.33 | 20.54 | 19.97 |
| 5 | 21.08 | 20.35 | 20.69 | 19.92 |
| 6 | 19.44 | 19.43 | 19.00 | 18.92 |
| 7 | 19.46 | 19.44 | 19.23 | 19.17 |

## 5. Results

Table 4 shows the simulation results of each scenario.

### 5.1. Control accuracy of MPC controller for multiple rooms

In our previous study [44], we researched the control results of the proposed MPC and PID control in terms of control accuracy, energy consumption, and hydraulic stability. In this subsection, we only discuss the control accuracy. We take Scenarios 1 and 2 as examples to analyze the control accuracy of the MPC controller for multiple rooms. Based on Table 4, the energy consumption of rooms without and with MPC

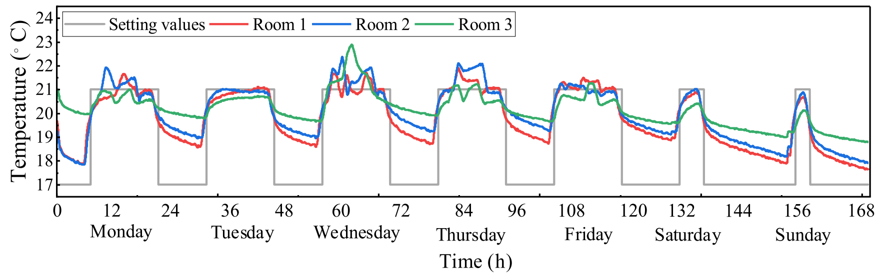


**Fig. 8.** Controlled indoor temperatures of Rooms 1 to 3 from 12th to December 18, 2022.

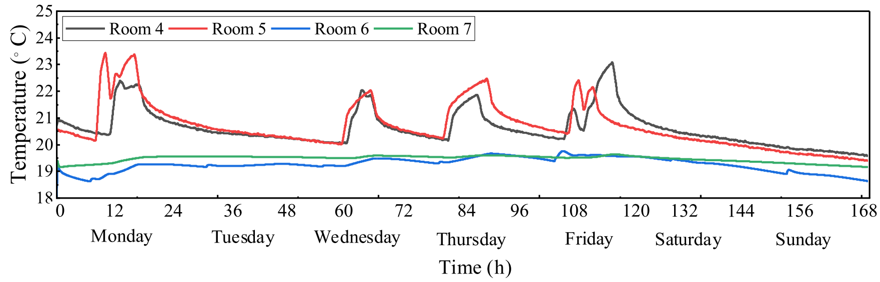


**Fig. 9.** Simulated indoor temperatures of Rooms 4 to 7 from 12 to December 18, 2022. Rooms 6 and 7 are corridors spaces.

controllers is 212.01 kWh and 192.72 kWh, respectively. Applying MPC and lower temperature setpoints for rooms during nonworking hours can save 9.1 % of heating energy for two reasons. Most significantly, lower temperature setpoints for the office rooms during nonworking hours reduce heat demand directly. Secondly, the MPC can achieve good control accuracy, for example, reducing overshoots, causing additional reduction in heating consumption. The details of the average indoor temperature of each room are shown in Table 5.

Fig. 8 shows the controlled one-week indoor temperature of three office rooms where MPC has been applied in Scenario 2. Fig. 9 shows the simulated indoor temperature of the other four rooms for one week, including two office rooms without radiators and two corridor spaces with radiators. The sampling time is 1 min.

The control effect of the MPC controller for Rooms 1 to 3 is good, with average accuracy ($P_{satisfied}$) of 91.7 % during working hours, as shown in Table 4. This means the temperature can be maintained within $\pm 1$ °C of setpoints most of the time. The temperatures during nonworking hours are above 17 °C all the time. The first reason for this is that weather was not extremely cold during the simulation period. The second reason is that heat transfer from the remaining part of the building maintains the temperature of the office rooms at a higher level than the setpoints during nonworking hours, as heating cannot be switched off for the whole building. The temperature peaks were caused by indoor thermal gains, such as people, lights, and equipment. The temperature of Rooms 4 and 5 is maintained at a satisfactory range during working hours. Temperatures in Rooms 6 and 7 are maintained above 17 °C all day. In conclusion, the MPC with an internal predictive model, as designed in this study, demonstrates applicability to temperature control in multiple rooms with good control accuracy.

**Table 6**
The total cost of Scenario 4 with different capacities of ASHP.

| The capacity of ASHP (Percentage of maximum demand) | Heat consumption (kWh) and proportion (%) | |
|---|---|---|
| | ASHP | DH |
| 60 % | 159.6/83.1 % | 32.5/16.9 % |
| 70 % | 170.0/88.5 % | 22.0/11.5 % |
| 80 % | 178.9/93.1 % | 13.2/6.9 % |

### 5.2. Analysis of optimal heat supply schemes

We consider Scenario 4 to analyze the cost savings when applying the optimal heat supply method to the demand side with various energy types. In our case, there are two types of energy: heat generated from ASHP and DH. Based on Table 4, applying the optimal heat supply method in Scenario 4 can save 20.9 % in costs compared to Scenario 2, using DH only. The cost-saving potential is large, especially when applying the method to the entire building.

There are two factors affecting the optimal heat supply schemes: dynamic heat price and the capacity of ASHP. Table 6 shows the percentage of supplied heat of ASHP and DH when choosing the different capacities of ASHP.

When we increase the capacity of ASHP, the percentage of heat provided by ASHP increases because the heat price of ASHP is lower than the heat price of DH most of the time. At this time, using more heat generated from ASHP is more cost-effective. However, as the COP factor of ASHP decreases in colder temperatures, a combination of high electricity price and cold outdoor temperature makes ASHP heating more expensive than DH. Fig. 10 shows one-day provided heat by ASHP and DH when the capacity of ASHP is 70 % of the maximum demand. The sampling time is 15 min.

The capacity of ASHP is 1546 W, marked with a grey dashed line in Fig. 10. The heat supplied by the ASHP, marked with a blue dotted line reaches full capacity only for a fraction of the time when demand is high and the ASHP heat price is lower than the DH price, such as the period from 7:15 to 8:00. During these hours, the ASHP must be supplemented by DH. A combination of low COP factors (due to cold weather) and high electricity prices makes the ASHP heat price higher than the DH price, such as the time from 14:00 to 20:00. During these hours, DH is used as the primary heat source supplemented by the ASHP only when the maximal DH capacity is reduced.

The heat supply problem will become more complex with various heat sources, such as the ground source heat pump, solar heat and power, electric boiler, and heat storage. With any configuration, optimization can minimize the heating costs for each time step considering

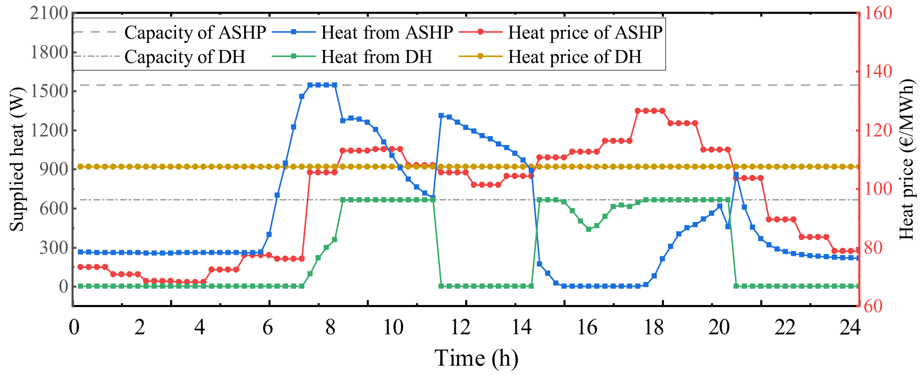


**Fig. 10.** Supplied heat on December 13, 2022.

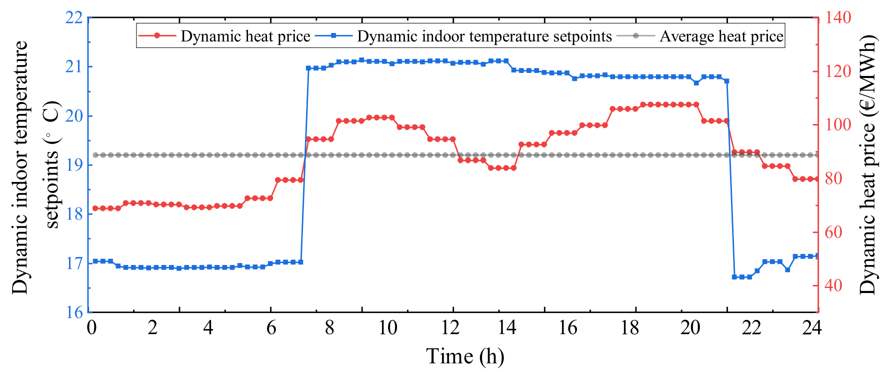


(a) Office rooms

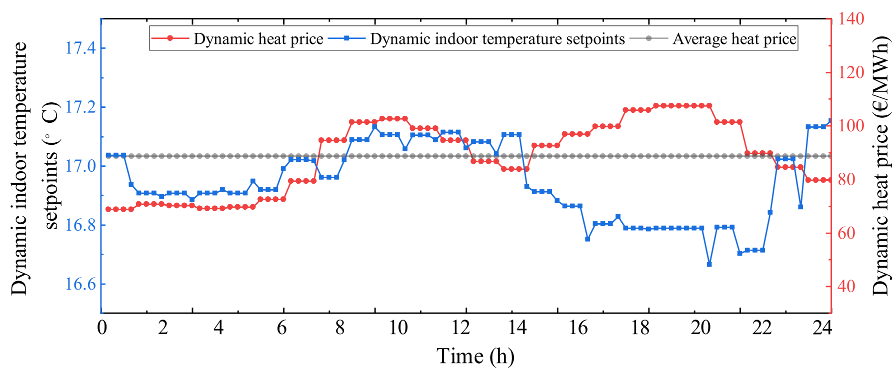


(b) Corridor

**Fig. 11.** Heat prices and indoor temperature setpoints on December 15, 2022.

all variable price factors and production constraints simultaneously [47].

### 5.3. Analysis of dynamic indoor temperature setpoints

We consider Scenario 5 to analyze dynamic indoor temperature setpoints based on dynamic heat prices using fuzzy logic. Fig. 11 shows one-day dynamic indoor temperature setpoints of the office rooms and corridor spaces on December 15, 2022. The sampling time is 15 min.

Typically, the dynamic heat price tends to be cheap during nonworking hours and expensive during working hours. Thus, the average heat price is lower than the actual dynamic heat price during working hours and higher than during nonworking hours. We can find a general rule from Fig. 11: the indoor temperature setpoints tend to increase to store more heat when the dynamic heat price is low and decrease when the dynamic heat price is high. But this rule does not always work because the increase or decrease of indoor temperature in the current moment also depends on the change between heat price in the next and present moments, already introduced in Subsection 4.2.

Based on Fig. 11, for office rooms, the indoor temperature setpoints vary from 20.6 °C to 21.2 °C during working hours and 16.6 °C–17.2 °C during nonworking hours. The indoor temperature setpoints for the corridor spaces vary from 16.6 °C to 17.2 °C. The flexible indoor temperature setpoints can shave heat demand peaks by utilizing the heat storage characteristics of the building and the dynamic heat prices, reducing heating demand and costs. For example, based on Table 4, compared to fixed temperature setpoints adopted in Scenario 4, introducing dynamic indoor temperature setpoints based on fuzzy logic can save 16.0 % of heat energy and 12.6 % of total cost.

## 6. Conclusions

In this study, an integrated DR method was developed to maintain thermal comfort and save heating energy and cost for the demand side.

In the optimization layer, fuzzy logic was proposed to adjust indoor temperature setpoints based on dynamic heat prices and the optimal heat supply method was used when multiple heat sources were applied. In the control layer, a multi-objective MPC approach, incorporating a simple internal predictive model for forecasting indoor temperatures, was employed to regulate the indoor temperature of multiple rooms. We built a multiple rooms model in CARNOT Toolbox and used this model to verify the feasibility of the proposed method. The conclusions are summarized below:

(1) The CARNOT Toolbox can be used to build models for multiple rooms to simulate the indoor temperature with sufficient accuracy. CARNOT Toolbox is a good and flexible tool for building models to simulate parameters or analyze the properties of the demand side, including a single room, multiple rooms, or even a whole building.
(2) The supplied heat for rooms without and with the MPC controller were 212.01 kWh and 192.72 kWh, respectively. Applying MPC to the rooms can save 9.1 % heating energy, meaning intermittent heating combined with suitable control technology has significant energy-saving potential, especially for commercial buildings with working and nonworking hours.
(3) The multi-objective MPC can demonstrate good control accuracy for indoor temperature control in multiple rooms, whether the indoor temperature setpoints are fixed or dynamic, with a satisfaction percentage of 91.7 % and 88.3 % during working hours.
(4) Fuzzy logic can be successfully applied to adjust indoor temperature setpoints based on dynamic heat prices to increase the flexibility of energy usage by utilizing the building's heat storage capacity, with 16.0 % energy saving and 12.6 % cost saving.
(5) Applying the optimal heat supply method for multiple rooms heated by ASHP and DH can fully utilize the different energy-supplied systems considering the dynamic electricity and heat prices to achieve minimum cost, with a cost-saving percentage of 20.9 %.

In this study, the optimization of heat supply considered only two heat sources. However, the model can be extended to include more complex configurations for heat supply. For example, ground source heat, solar heat and power, electric boilers, and heat storage can be included. Studying performance in such more complex configurations to balance both heat and electricity supply and demand is a topic for further studies. In addition, this study is a preliminary exploration of using fuzzy logic to determine indoor temperature setpoints. Further research is needed, such as investigating different fuzzy methods and membership functions to find the best combination.

## CRediT authorship contribution statement

**Pengmin Hua:** Writing – review & editing, Writing – original draft, Software, Methodology, Formal analysis, Conceptualization. **Haichao Wang:** Writing – review & editing, Funding acquisition. **Zichan Xie:** Writing – review & editing. **Risto Lahdelma:** Writing – review & editing, Supervision, Methodology, Formal analysis, Conceptualization.

## Declaration of competing interest

The authors declare that they have no known competing financial interests or personal relationships that could have appeared to influence the work reported in this paper

## Data availability

Data will be made available on request.

## Acknowledgements

This study was supported by National Key R&D Program of China (2021YFE0116200) and the Academy Research Fellow project and allocated initial funding for research costs – Spatiotemporal dynamic simulation of the thermal energy storage (TES) assisted heating network and optimization for indoor temperature control (NO. 334205 and NO.358055). The authors would like to thank the Walter Ahlström Foundation for financially supporting this research (https://walterahlstrom.fi/).

## Appendix A

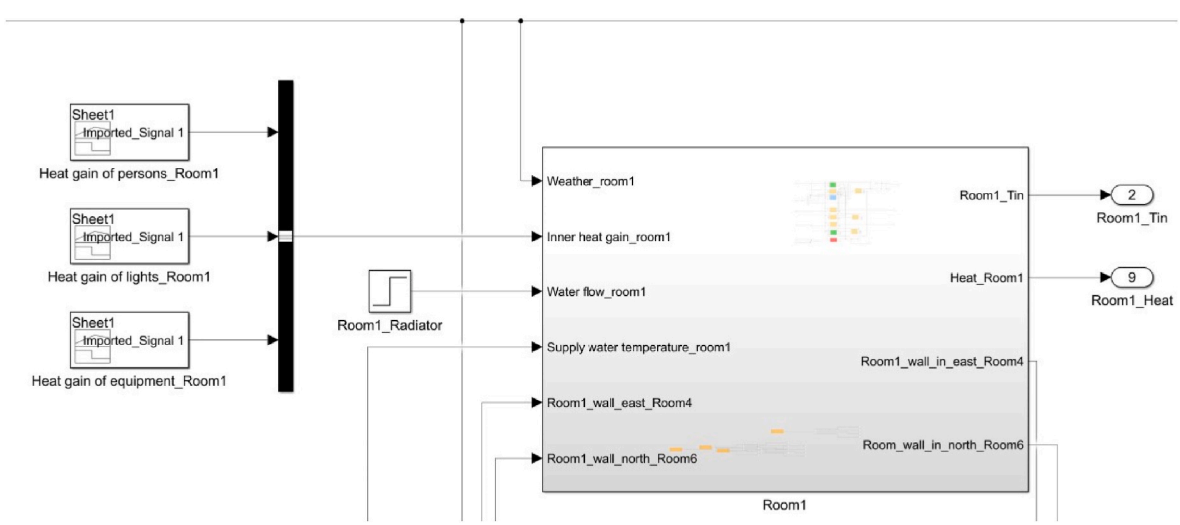

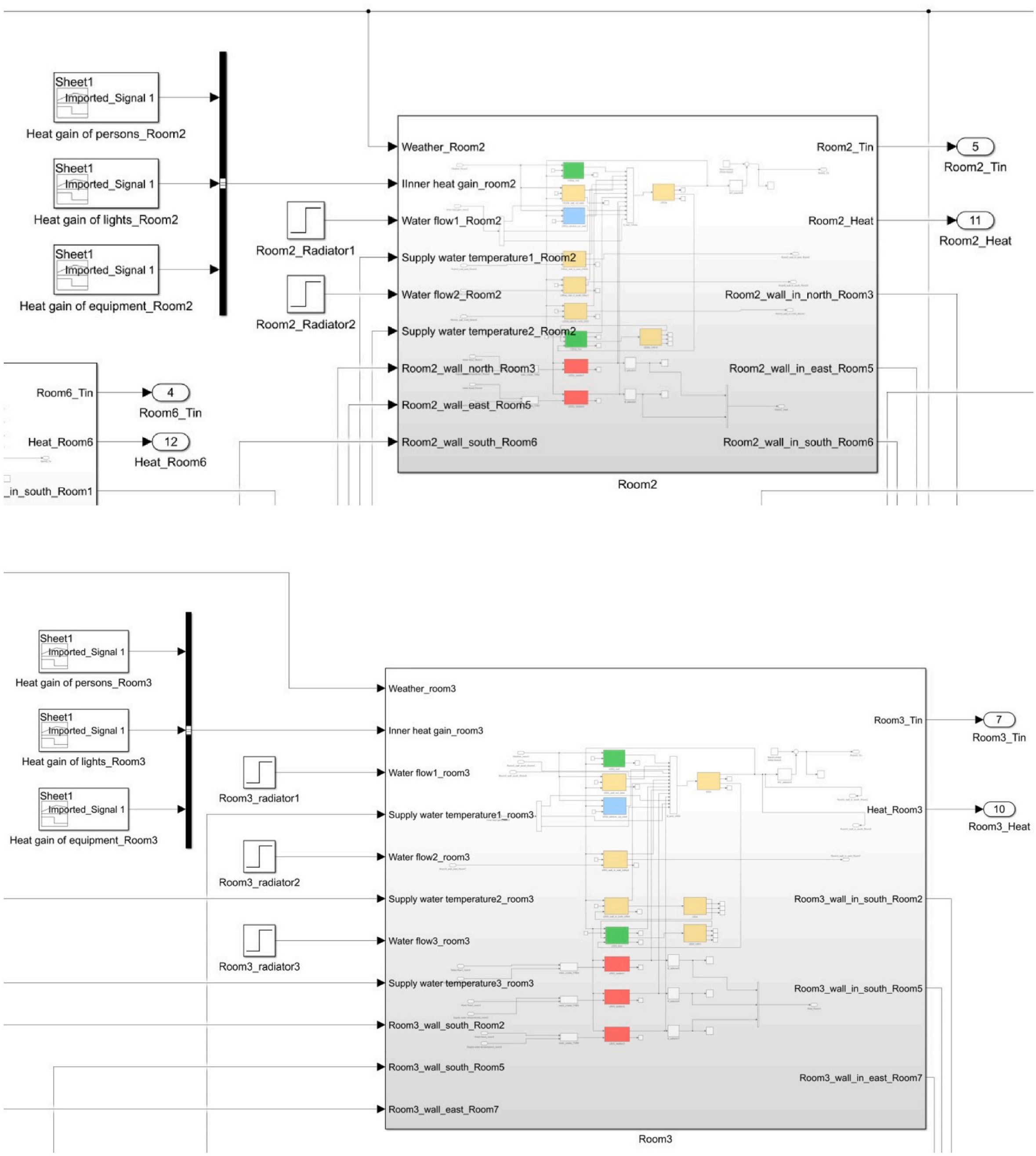
Sheet1
Imported_Signal 1
Heat gain of persons_Room2
Sheet1
Imported_Signal 1
Heat gain of lights_Room2
Sheet1
Imported_Signal 1
Heat gain of equipment_Room2
Room2_Radiator1
Room2_Radiator2
Weather_Room2
IInner heat gain_room2
Water flow1_Room2
Supply water temperature1_Room2
Water flow2_Room2
Supply water temperature2_Room2
Room2_wall_north_Room3
Room2_wall_east_Room5
Room2_wall_south_Room6
Room2_Tin
Room2_Heat
Room2_wall_in_north_Room3
Room2_wall_in_east_Room5
Room2_wall_in_south_Room6
Room2
5
Room2_Tin
11
Room2_Heat
Room6_Tin
4
Room6_Tin
Heat_Room6
12
Heat_Room6
_in_south_Room1
Sheet1
Imported_Signal 1
Heat gain of persons_Room3
Sheet1
Imported_Signal 1
Heat gain of lights_Room3
Sheet1
Imported_Signal 1
Heat gain of equipment_Room3
Room3_radiator1
Room3_radiator2
Room3_radiator3
Weather_room3
Inner heat gain_room3
Water flow1_room3
Supply water temperature1_room3
Water flow2_room3
Supply water temperature2_room3
Water flow3_room3
Supply water temperature3_room3
Room3_wall_south_Room2
Room3_wall_south_Room5
Room3_wall_east_Room7
Room3_Tin
Heat_Room3
Room3_wall_in_south_Room2
Room3_wall_in_south_Room5
Room3_wall_in_east_Room7
Room3
7
Room3_Tin
10
Room3_Heat

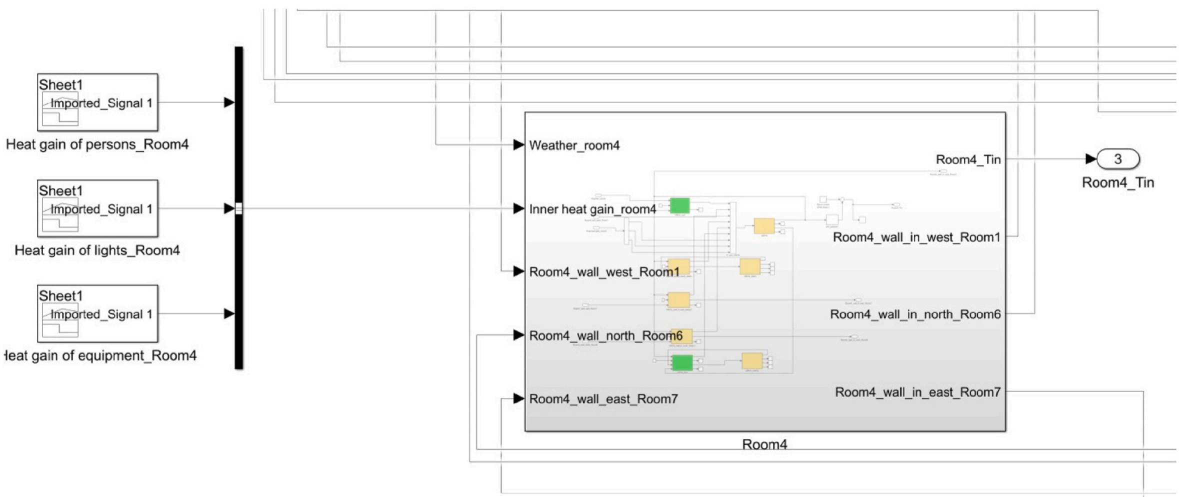
Sheet1
Imported_Signal 1
Heat gain of persons_Room4
Sheet1
Imported_Signal 1
Heat gain of lights_Room4
Sheet1
Imported_Signal 1
Heat gain of equipment_Room4
Weather_room4
Inner heat gain_room4
Room4_wall_west_Room1
Room4_wall_north_Room6
Room4_wall_east_Room7
Room4_Tin
Room4_wall_in_west_Room1
Room4_wall_in_north_Room6
Room4_wall_in_east_Room7
Room4
3
Room4_Tin

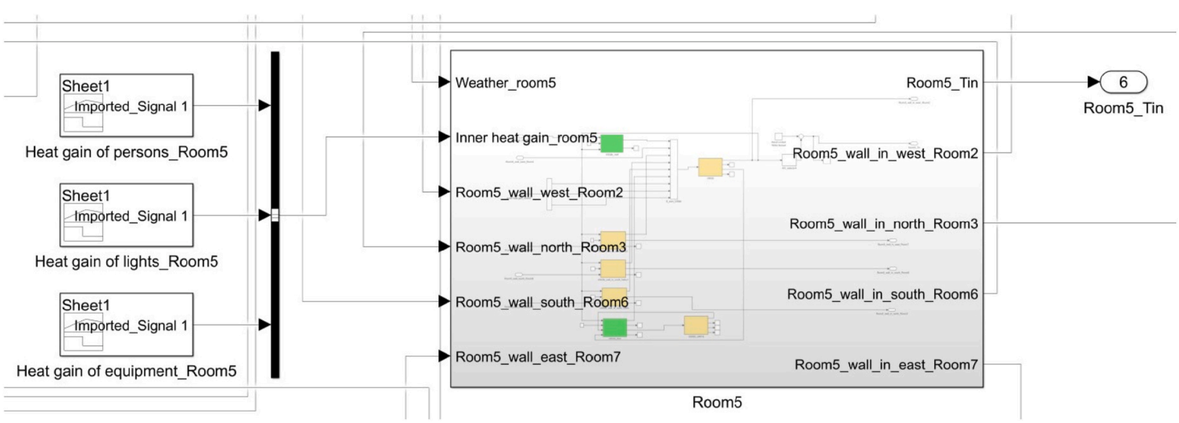
Sheet1
Imported_Signal 1
Heat gain of persons_Room5
Sheet1
Imported_Signal 1
Heat gain of lights_Room5
Sheet1
Imported_Signal 1
Heat gain of equipment_Room5
Weather_room5
Inner heat gain_room5
Room5_wall_west_Room2
Room5_wall_north_Room3
Room5_wall_south_Room6
Room5_wall_east_Room7
Room5_Tin
Room5_wall_in_west_Room2
Room5_wall_in_north_Room3
Room5_wall_in_south_Room6
Room5_wall_in_east_Room7
Room5
6
Room5_Tin

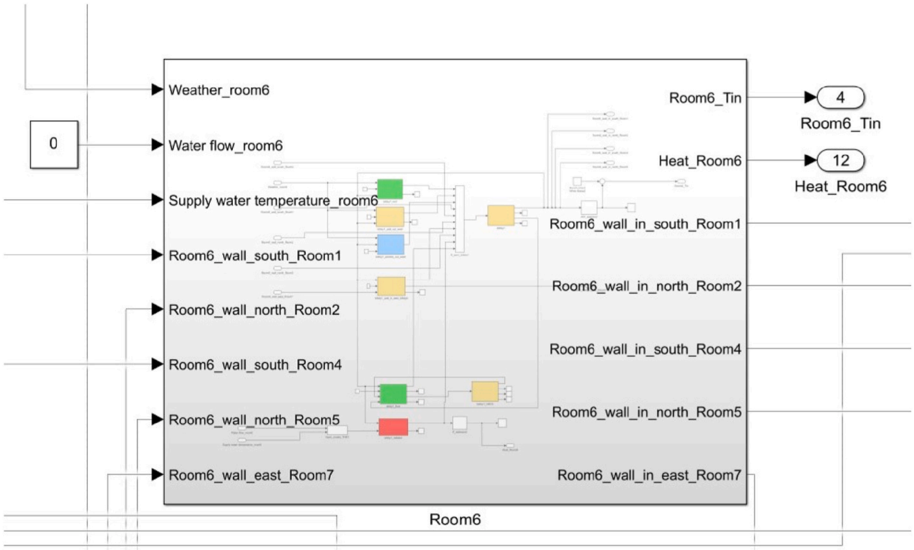


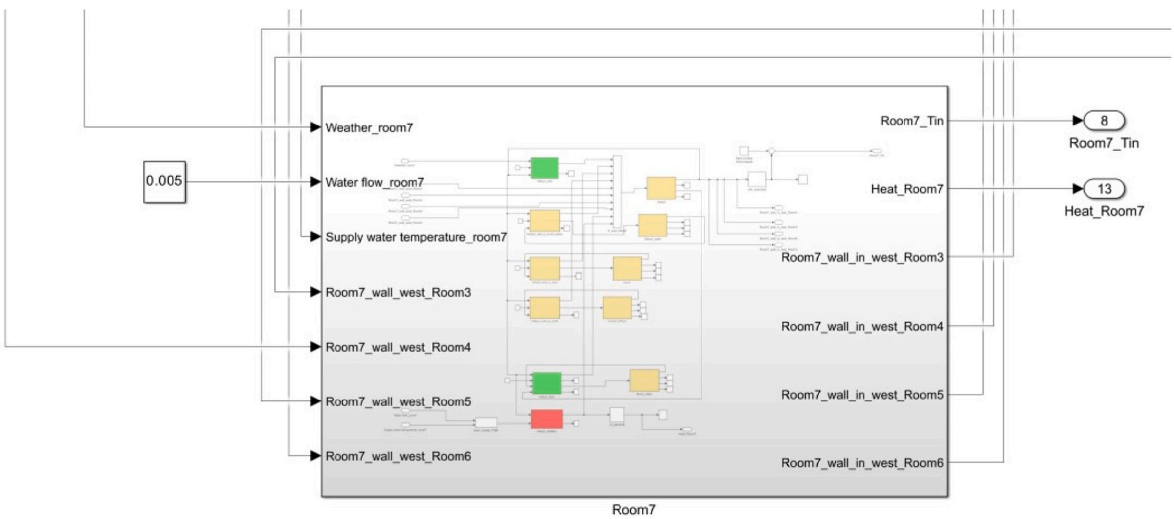


## Appendix B

$$Y(k) = \Omega X(k) = \Omega \Phi x(k) + \Omega G_y \Delta U(k) + \Omega \Gamma u(k-1) + \Omega N \Delta D(k) + \Omega M d(k-1). \tag{7}$$

Here,

$$Y(k) = \begin{bmatrix} y(k+1|k) \\ y(k+2|k) \\ \vdots \\ y(k+N_c|k) \\ y(k+N_c+1|k) \\ \vdots \\ y(k+N_p|k) \end{bmatrix}; X(k) = \begin{bmatrix} x(k+1|k) \\ x(k+2|k) \\ \vdots \\ x(k+N_c|k) \\ x(k+N_c+1|k) \\ \vdots \\ x(k+N_p|k) \end{bmatrix}; \Delta U(k) = \begin{bmatrix} \Delta u(k|k) \\ \Delta u(k+1|k) \\ \vdots \\ \Delta u(k+N_c-1|k) \end{bmatrix}; \Delta D(k) = \begin{bmatrix} \Delta d(k|k) \\ \Delta d(k+1|k) \\ \vdots \\ \Delta d(k+N_p-1|k) \end{bmatrix};$$

$$\Omega = \begin{bmatrix} C_d & 0 & \dots & 0 \\ 0 & C_d & \dots & 0 \\ 0 & 0 & \ddots & 0 \\ 0 & 0 & \dots & C_d \end{bmatrix}; \Phi = \begin{bmatrix} A_d \\ A_d^2 \\ \vdots \\ A_d^{N_c} \\ A_d^{N_c+1} \\ \vdots \\ A_d^{N_p} \end{bmatrix}; \Gamma = \begin{bmatrix} B_d \\ A_d B_d + B_d \\ \vdots \\ \sum_{i=0}^{N_c-1} A_d^i B_d \\ \sum_{i=0}^{N_c} A_d^i B_d \\ \vdots \\ \sum_{i=0}^{N_p-1} A_d^i B_d \end{bmatrix}; Gy = \begin{bmatrix} B_d & 0 & \cdots & 0 \\ (A_d+I)B_d & B_d & \cdots & 0 \\ \vdots & \vdots & \vdots & \vdots \\ \sum_{i=0}^{N_c-1} A_d^i B_d & \cdots & \cdots & B_d \\ \sum_{i=0}^{N_c} A_d^i B_d & \cdots & \cdots & (A_d+I)B_d \\ \vdots & \vdots & \vdots & \vdots \\ \sum_{i=0}^{N_p-1} A_d^i B_d & \cdots & \cdots & \sum_{i=0}^{N_p-N_c} A_d^i B_d \end{bmatrix};$$

$$M = \begin{bmatrix} E_d \\ A_d E_d \\ \vdots \\ \sum_{i=0}^{N_c-1} A_d^i E_d \\ \sum_{i=0}^{N_c} A_d^i E_d \\ \vdots \\ \sum_{i=0}^{N_p-1} A_d^i E_d \end{bmatrix}; N = \begin{bmatrix} E_d & \cdots & \cdots & \cdots & 0 \\ (A_d+I)E_d & E_d & \cdots & \cdots & 0 \\ \vdots & \vdots & \vdots & \vdots & \vdots \\ \sum_{i=0}^{N_c-1} A_d^i E_d & \cdots & E_d & \cdots & 0 \\ \sum_{i=0}^{N_c} A_d^i E_d & \cdots & \cdots & E_d & 0 \\ \vdots & \vdots & \vdots & \vdots & \vdots \\ \sum_{i=0}^{N_p-1} A_d^i E_d & \cdots & \cdots & \cdots & E_d \end{bmatrix}.$$

## Appendix C

The internal predictive model for multiple rooms in this study is shown as follows.

Room1:

$$\frac{dT_{in,1}}{d\tau} = -\frac{U_{win,1}A_{win,1} + U_{roof,ext,wall,1}A_{roof,ext,wall,1} + U_{\text{int},wall,1,6}A_{\text{int},wall,1,6} + U_{\text{int},wall,1,4}A_{\text{int},wall,1,4} + U_{\text{int},wall,1,adj1}A_{\text{int},wall,1,adj1} + U_{\text{int},wall,1,adj5}A_{\text{int},wall,1,adj5}}{\rho_{in,1}c_{in,1}V_{in,1}}T_{in,1}$$
$$+ \frac{U_{\text{int},wall,1,4}A_{\text{int},wall,1,4}}{\rho_{in,1}c_{in,1}V_{in,1}}T_{in,4} + \frac{U_{\text{int},wall,1,6}A_{\text{int},wall,1,6}}{\rho_{in,1}c_{in,1}V_{in,1}}T_{in,6} + \frac{1}{\rho_{in,1}c_{in,1}V_{in,1}}Qrad,1 + \frac{U_{win,1}A_{win,1} + U_{roof,ext,wall,1}A_{roof,ext,wall,1}}{\rho_{in,1}c_{in,1}V_{in,1}}T_{out} + \frac{\alpha_1 A_{win,1}}{\rho_{in,1}c_{in,1}V_{in,1}}I_{solar}$$
$$+ \frac{U_{\text{int},wall,1,adj1}A_{\text{int},wall,1,adj1}}{\rho_{in,1}c_{in,1}V_{in,1}}T_{in,adj1} + \frac{U_{\text{int},wall,1,adj5}A_{\text{int},wall,1,adj5}}{\rho_{in,1}c_{in,1}V_{in,1}}T_{in,adj5}$$

Room2

$$\frac{dT_{in,2}}{d\tau} = -\frac{U_{win,2}A_{win,2} + U_{roof,ext,wall,2}A_{roof,ext,wall,2} + U_{\text{int},wall,2,6}A_{\text{int},wall,2,6} + U_{\text{int},wall,2,5}A_{\text{int},wall,2,5} + U_{\text{int},wall,2,3}A_{\text{int},wall,2,3} + U_{\text{int},wall,2,adj6}A_{\text{int},wall,2,adj6}}{\rho_{in,2}c_{in,2}V_{in,2}}T_{in,2}$$
$$+ \frac{U_{\text{int},wall,2,3}A_{\text{int},wall,2,3}}{\rho_{in,2}c_{in,2}V_{in,2}}T_{in,3} + \frac{U_{\text{int},wall,2,5}A_{\text{int},wall,2,5}}{\rho_{in,2}c_{in,2}V_{in,2}}T_{in,5} + \frac{U_{\text{int},wall,2,6}A_{\text{int},wall,2,6}}{\rho_{in,2}c_{in,2}V_{in,2}}T_{in,6} + \frac{1}{\rho_{in,2}c_{in,2}V_{in,2}}Q_{rad,2} + \frac{U_{win,2}A_{win,2} + U_{roof,ext,wall,2}A_{roof,ext,wall,2}}{\rho_{in,2}c_{in,2}V_{in,2}}T_{out}$$
$$+ \frac{\alpha_2 A_{win,2}}{\rho_{in,2}c_{in,2}V_{in,2}}I_{solar} + \frac{U_{\text{int},wall,2,adj6}A_{\text{int},wall,2,adj6}}{\rho_{in,2}c_{in,2}V_{in,2}}T_{in,adj6}$$

Room3

$$\frac{dT_{in,3}}{d\tau}= -\frac{U_{win,3}A_{win,3}+U_{roof,ext,wall,3}A_{roof,ext,wall,3}+U_{\mathrm{int},wall,2,3}A_{\mathrm{int},wall,2,3}+U_{\mathrm{int},wall,3,5}A_{\mathrm{int},wall,3,5}+U_{\mathrm{int},wall,3,7}A_{\mathrm{int},wall,3,7}+U_{\mathrm{int},wall,3,adj4}A_{\mathrm{int},wall,3,adj4}+U_{\mathrm{int},wall,3,adj6}A_{\mathrm{int},wall,3,adj6}}{\rho_{in,3}c_{in,3}V_{in,3}}T_{in,3} + \frac{U_{\mathrm{int},wall,2,3}A_{\mathrm{int},wall,2,3}}{\rho_{in,3}c_{in,3}V_{in,3}}T_{in,2}+\frac{U_{\mathrm{int},wall,3,5}A_{\mathrm{int},wall,3,5}}{\rho_{in,3}c_{in,3}V_{in,3}}T_{in,5}+\frac{U_{\mathrm{int},wall,3,7}A_{\mathrm{int},wall,3,7}}{\rho_{in,3}c_{in,3}V_{in,3}}T_{in,7}+\frac{1}{\rho_{in,3}c_{in,3}V_{in,3}}Q_{rad,3}+\frac{U_{win,3}A_{win,3}+U_{roof,ext,wall,3}A_{roof,ext,wall,3}}{\rho_{in,3}c_{in,3}V_{in,3}}T_{out}+\frac{\alpha_3A_{win,3}}{\rho_{in,3}c_{in,3}V_{in,3}}I_{solar} + \frac{U_{\mathrm{int},wall,3,adj4}A_{\mathrm{int},wall,3,adj4}}{\rho_{in,3}c_{in,3}V_{in,3}}T_{in,adj4}+\frac{U_{\mathrm{int},wall,3,adj6}A_{\mathrm{int},wall,3,adj6}}{\rho_{in,3}c_{in,3}V_{in,3}}T_{in,adj6}$$

Room4

$$\frac{dT_{in,4}}{d\tau}= -\frac{U_{roof,4}A_{roof,4}+U_{\mathrm{int},wall,1,4}A_{\mathrm{int},wall,1,4}+U_{\mathrm{int},wall,4,6}A_{\mathrm{int},wall,4,6}+U_{\mathrm{int},wall,4,7}A_{\mathrm{int},wall,4,7}+U_{\mathrm{int},wall,4,adj1}A_{\mathrm{int},wall,4,adj1}+U_{\mathrm{int},wall,4,adj5}A_{\mathrm{int},wall,4,adj5}}{\rho_{in,4}c_{in,4}V_{in,4}}T_{in,4} + \frac{U_{\mathrm{int},wall,1,4}A_{\mathrm{int},wall,1,4}}{\rho_{in,4}c_{in,4}V_{in,4}}T_{in,1}+\frac{U_{\mathrm{int},wall,4,6}A_{\mathrm{int},wall,4,6}}{\rho_{in,4}c_{in,4}V_{in,4}}T_{in,6}+\frac{U_{\mathrm{int},wall,4,7}A_{\mathrm{int},wall,4,7}}{\rho_{in,4}c_{in,4}V_{in,4}}T_{in,7}+\frac{U_{roof,4}A_{roof,4}}{\rho_{in,4}c_{in,4}V_{in,4}}T_{out}+\frac{U_{\mathrm{int},wall,4,adj1}A_{\mathrm{int},wall,4,adj1}}{\rho_{in,4}c_{in,4}V_{in,4}}T_{in,adj1} + \frac{U_{\mathrm{int},wall,4,adj5}A_{\mathrm{int},wall,4,adj5}}{\rho_{in,4}c_{in,4}V_{in,4}}T_{in,adj5}$$

Room5

$$\frac{dT_{in,5}}{d\tau}= -\frac{U_{roof,5}A_{roof,5}+U_{\mathrm{int},wall,2,5}A_{\mathrm{int},wall,2,5}+U_{\mathrm{int},wall,5,6}A_{\mathrm{int},wall,5,6}+U_{\mathrm{int},wall,5,7}A_{\mathrm{int},wall,5,7}+U_{\mathrm{int},wall,3,5}A_{\mathrm{int},wall,3,5}+U_{\mathrm{int},wall,5,adj6}A_{\mathrm{int},wall,5,adj6}}{\rho_{in,5}c_{in,5}V_{in,5}}T_{in,5} + \frac{U_{\mathrm{int},wall,2,5}A_{\mathrm{int},wall,2,5}}{\rho_{in,5}c_{in,5}V_{in,5}}T_{in,2}+\frac{U_{\mathrm{int},wall,3,5}A_{\mathrm{int},wall,3,5}}{\rho_{in,5}c_{in,5}V_{in,5}}T_{in,3}+\frac{U_{\mathrm{int},wall,5,6}A_{\mathrm{int},wall,5,6}}{\rho_{in,5}c_{in,5}V_{in,5}}T_{in,6}+\frac{U_{\mathrm{int},wall,5,7}A_{\mathrm{int},wall,5,7}}{\rho_{in,5}c_{in,5}V_{in,5}}T_{in,7}+\frac{U_{roof,5}A_{roof,5}}{\rho_{in,5}c_{in,5}V_{in,5}}T_{out}+\frac{U_{\mathrm{int},wall,5,adj6}A_{\mathrm{int},wall,5,adj6}}{\rho_{in,5}c_{in,5}V_{in,5}}T_{in,adj6}$$

Room6:

$$\frac{dT_{in,6}}{d\tau}= -\frac{U_{win,6}A_{win,6}+U_{roof,ext,wall,6}A_{roof,ext,wall,6}+U_{\mathrm{int},wall,1,6}A_{\mathrm{int},wall,1,6}+U_{\mathrm{int},wall,2,6}A_{\mathrm{int},wall,2,6}+U_{\mathrm{int},wall,4,6}A_{\mathrm{int},wall,4,6}+U_{\mathrm{int},wall,5,6}A_{\mathrm{int},wall,5,6}+U_{\mathrm{int},wall,6,7}A_{\mathrm{int},wall,6,7}+U_{\mathrm{int},wall,6,adj5}A_{\mathrm{int},wall,6,adj5}}{\rho_{in,6}c_{in,6}V_{in,6}}T_{in,6}+\frac{U_{\mathrm{int},wall,1,6}A_{\mathrm{int},wall,1,6}}{\rho_{in,6}c_{in,6}V_{in,6}}T_{in,1} +\frac{U_{\mathrm{int},wall,2,6}A_{\mathrm{int},wall,2,6}}{\rho_{in,6}c_{in,6}V_{in,6}}T_{in,2}+\frac{U_{\mathrm{int},wall,4,6}A_{\mathrm{int},wall,4,6}}{\rho_{in,6}c_{in,6}V_{in,6}}T_{in,4}+\frac{U_{\mathrm{int},wall,5,6}A_{\mathrm{int},wall,5,6}}{\rho_{in,6}c_{in,6}V_{in,6}}T_{in,5}+\frac{U_{\mathrm{int},wall,6,7}A_{\mathrm{int},wall,6,7}}{\rho_{in,6}c_{in,6}V_{in,6}}T_{in,7}+\frac{1}{\rho_{in,6}c_{in,6}V_{in,6}}Q_{rad,6}+\frac{U_{win,6}A_{win,6}+U_{roof,ext,wall,6}A_{roof,ext,wall,6}}{\rho_{in,6}c_{in,6}V_{in,6}}T_{out}+\frac{\alpha_6A_{win,6}}{\rho_{in,6}c_{in,6}V_{in,6}}I_{solar}+\frac{U_{\mathrm{int},wall,6,adj5}A_{\mathrm{int},wall,6,adj5}}{\rho_{in,6}c_{in,6}V_{in,6}}T_{in,adj5}$$

Room7

$$\frac{dT_{in,7}}{d\tau}= -\frac{U_{roof,7}A_{roof,7}+U_{\mathrm{int},wall,3,7}A_{\mathrm{int},wall,3,7}+U_{\mathrm{int},wall,5,7}A_{\mathrm{int},wall,5,7}+U_{\mathrm{int},wall,6,7}A_{\mathrm{int},wall,6,7}+U_{\mathrm{int},wall,4,7}A_{\mathrm{int},wall,4,7}+U_{\mathrm{int},wall,7,adj1}A_{\mathrm{int},wall,7,adj1}+U_{\mathrm{int},wall,7,adj2}A_{\mathrm{int},wall,7,adj2}+U_{\mathrm{int},wall,7,adj3}A_{\mathrm{int},wall,7,adj3}}{\rho_{in,7}c_{in,7}V_{in,7}}T_{in,7}+\frac{U_{\mathrm{int},wall,3,7}A_{\mathrm{int},wall,3,7}}{\rho_{in,7}c_{in,7}V_{in,7}}T_{in,3} +\frac{U_{\mathrm{int},wall,4,7}A_{\mathrm{int},wall,4,7}}{\rho_{in,7}c_{in,7}V_{in,7}}T_{in,4}+\frac{U_{\mathrm{int},wall,5,7}A_{\mathrm{int},wall,5,7}}{\rho_{in,7}c_{in,7}V_{in,7}}T_{in,5}+\frac{U_{\mathrm{int},wall,6,7}A_{\mathrm{int},wall,6,7}}{\rho_{in,7}c_{in,7}V_{in,7}}T_{in,6}+\frac{1}{\rho_{in,7}c_{in,7}V_{in,7}}Q_{rad,7}+\frac{U_{roof,7}A_{roof,7}}{\rho_{in,7}c_{in,7}V_{in,7}}T_{out}+\frac{U_{\mathrm{int},wall,7,adj1}A_{\mathrm{int},wall,7,adj1}}{\rho_{in,7}c_{in,7}V_{in,7}}T_{in,adj1}+\frac{U_{\mathrm{int},wall,7,adj2}A_{\mathrm{int},wall,7,adj2}}{\rho_{in,7}c_{in,7}V_{in,7}}T_{in,adj2}+\frac{U_{\mathrm{int},wall,7,adj3}A_{\mathrm{int},wall,7,adj3}}{\rho_{in,7}c_{in,7}V_{in,7}}T_{in,adj3}$$

The matrix $A$, $B$, $C$, $E$ of the state space representation for the multiple room are show as follows.

$$A_{row1}=\begin{bmatrix} -\frac{\begin{array}{c}U_{win,1}A_{win,1}+U_{roof,ext,wall,1}A_{roof,ext,wall,1}+\\ U_{\mathrm{int},wall,1,6}A_{\mathrm{int},wall,1,6}+U_{\mathrm{int},wall,1,4}A_{\mathrm{int},wall,1,4}+\\ U_{\mathrm{int},wall,1,adj1}A_{\mathrm{int},wall,1,adj1}+U_{\mathrm{int},wall,1,adj5}A_{\mathrm{int},wall,1,adj5}\end{array}}{\rho_{in,1}c_{in,1}V_{in,1}} & 0 & 0 & \frac{U_{\mathrm{int},wall,1,4}A_{\mathrm{int},wall,1,4}}{\rho_{in,1}c_{in,1}V_{in,1}} & 0 & \frac{U_{\mathrm{int},wall,1,6}A_{\mathrm{int},wall,1,6}}{\rho_{in,1}c_{in,1}V_{in,1}} & 0 \end{bmatrix}$$

$$A_{row2}=\begin{bmatrix} 0 & -\frac{\begin{array}{c}U_{win,2}A_{win,2}+U_{roof,ext,wall,2}A_{roof,ext,wall,2}+\\ U_{\mathrm{int},wall,2,6}A_{\mathrm{int},wall,2,6}+U_{\mathrm{int},wall,2,5}A_{\mathrm{int},wall,2,5}+\\ U_{\mathrm{int},wal,2,3}A_{\mathrm{int},wall,2,3}+U_{\mathrm{int},wall,2,adj6}A_{\mathrm{int},wall,2,adj6}\end{array}}{\rho_{in,2}c_{in,2}V_{in,2}} & \frac{U_{\mathrm{int},wall,2,3}A_{\mathrm{int},wall,2,3}}{\rho_{in,2}c_{in,2}V_{in,2}} & 0 & \frac{U_{\mathrm{int},wall,2,5}A_{\mathrm{int},wall,2,5}}{\rho_{in,2}c_{in,2}V_{in,2}} & \frac{U_{\mathrm{int},wall,2,6}A_{\mathrm{int},wall,2,6}}{\rho_{in,2}c_{in,2}V_{in,2}} & 0 \end{bmatrix}$$

$$A_{row3}=\begin{bmatrix} 0 & \frac{U_{\mathrm{int},wall,2,3}A_{\mathrm{int},wall,2,3}}{\rho_{in,3}c_{in,3}V_{in,3}} & -\frac{\begin{array}{c}U_{win,3}A_{win,3}+U_{roof,ext,wall,3}A_{roof,ext,wall,3}+\\ U_{\mathrm{int},wall,2,3}A_{\mathrm{int},wall,2,3}+U_{\mathrm{int},wall,3,5}A_{\mathrm{int},wall,3,5}+\\ U_{\mathrm{int},wall,3,7}A_{\mathrm{int},wall,3,7}+U_{\mathrm{int},wall,3,adj4}A_{\mathrm{int},wall,3,adj4}+\\ U_{\mathrm{int},wall,3,adj6}A_{\mathrm{int},wall,3,adj6}\end{array}}{\rho_{in,3}c_{in,3}V_{in,3}} & 0 & \frac{U_{\mathrm{int},wall,3,5}A_{\mathrm{int},wall,3,5}}{\rho_{in,3}c_{in,3}V_{in,3}} & 0 & \frac{U_{\mathrm{int},wall,3,7}A_{\mathrm{int},wall,3,7}}{\rho_{in,3}c_{in,3}V_{in,3}} \end{bmatrix}$$

$$A_{row4}=\begin{bmatrix} \frac{U_{\mathrm{int},wall,1,4}A_{\mathrm{int},wall,1,4}}{\rho_{in,4}c_{in,4}V_{in,4}} & 0 & 0 & -\frac{\begin{array}{c}U_{roof,ext,wall,4}A_{roof,ext,wall,4}+\\ U_{\mathrm{int},wall,1,4}A_{\mathrm{int},wall,1,4}+U_{\mathrm{int},wall,4,6}A_{\mathrm{int},wall,4,6}+\\ U_{\mathrm{int},wall,4,7}A_{\mathrm{int},wall,4,7}+U_{\mathrm{int},wall,4,adj1}A_{\mathrm{int},wall,4,adj1}+\\ U_{\mathrm{int},wall,4,adj5}A_{\mathrm{int},wall,4,adj5}\end{array}}{\rho_{in,4}c_{in,4}V_{in,4}} & 0 & \frac{U_{\mathrm{int},wall,4,6}A_{\mathrm{int},wall,4,6}}{\rho_{in,4}c_{in,4}V_{in,4}} & \frac{U_{\mathrm{int},wall,4,7}A_{\mathrm{int},wall,4,7}}{\rho_{in,4}c_{in,4}V_{in,4}} \end{bmatrix}$$

$$A_{row5}=\left[\begin{array}{ccccccc} 0 & \frac{U_{\mathrm{int},wall,2,5}A_{\mathrm{int},wall,2,5}}{\rho_{in,5}c_{in,5}V_{in,5}} & \frac{U_{\mathrm{int},wall,3,5}A_{\mathrm{int},wall,3,5}}{\rho_{in,5}c_{in,5}V_{in,5}} & 0 & -\frac{\begin{array}{c}U_{roof,ext,wall,5}A_{roof,ext,wall,5}+\\ U_{\mathrm{int},wall,2,5}A_{\mathrm{int},wall,2,5}+U_{\mathrm{int},wall,5,6}A_{\mathrm{int},wall,5,6}+\\ U_{\mathrm{int},wall,5,7}A_{\mathrm{int},wall,5,7}+U_{\mathrm{int},wall,3,5}A_{\mathrm{int},wall,3,5}+\\ U_{\mathrm{int},wall,5,adj6}A_{\mathrm{int},wall,5,adj6}\end{array}}{\rho_{in,5}c_{in,5}V_{in,5}} & \frac{U_{\mathrm{int},wall,5,6}A_{\mathrm{int},wall,5,6}}{\rho_{in,5}c_{in,5}V_{in,5}} & \frac{U_{\mathrm{int},wall,5,7}A_{\mathrm{int},wall,5,7}}{\rho_{in,5}c_{in,5}V_{in,5}} \end{array}\right]$$

$$A_{row6}=\left[\begin{array}{ccccccc} \frac{U_{\mathrm{int},wall,1,6}A_{\mathrm{int},wall,1,6}}{\rho_{in,6}c_{in,6}V_{in,6}} & \frac{U_{\mathrm{int},wall,2,6}A_{\mathrm{int},wall,2,6}}{\rho_{in,6}c_{in,6}V_{in,6}} & 0 & \frac{U_{\mathrm{int},wall,4,6}A_{\mathrm{int},wall,4,6}}{\rho_{in,6}c_{in,6}V_{in,6}} & \frac{U_{\mathrm{int},wall,5,6}A_{\mathrm{int},wall,5,6}}{\rho_{in,6}c_{in,6}V_{in,6}} & -\frac{\begin{array}{c}U_{win,6}A_{win,6}+U_{roof,ext,wall,6}A_{roof,ext,wall,6}+\\ U_{\mathrm{int},wall,1,6}A_{\mathrm{int},wall,1,6}+U_{\mathrm{int},wall,2,6}A_{\mathrm{int},wall,2,6}+\\ U_{\mathrm{int},wall,4,6}A_{\mathrm{int},wall,4,6}+U_{\mathrm{int},wall,5,6}A_{\mathrm{int},wall,5,6}+\\ U_{\mathrm{int},wall,6,7}A_{\mathrm{int},wall,6,7}+U_{\mathrm{int},wall,6,adj5}A_{\mathrm{int},wall,6,adj5}\end{array}}{\rho_{in,6}c_{in,6}V_{in,6}} & \frac{U_{\mathrm{int},wall,6,7}A_{\mathrm{int},wall,6,7}}{\rho_{in,6}c_{in,6}V_{in,6}} \end{array}\right]$$

$$A_{row7}=\left[\begin{array}{ccccccc} 0 & 0 & \frac{U_{\mathrm{int},wall,3,7}A_{\mathrm{int},wall,3,7}}{\rho_{in,7}c_{in,7}V_{in,7}} & \frac{U_{\mathrm{int},wall,4,7}A_{\mathrm{int},wall,4,7}}{\rho_{in,7}c_{in,7}V_{in,7}} & \frac{U_{\mathrm{int},wall,5,7}A_{\mathrm{int},wall,5,7}}{\rho_{in,7}c_{in,7}V_{in,7}} & \frac{U_{\mathrm{int},wall,6,7}A_{\mathrm{int},wall,6,7}}{\rho_{in,7}c_{in,7}V_{in,7}} & -\frac{\begin{array}{c}U_{roof,7}A_{roof,7}+U_{\mathrm{int},wall,3,7}A_{\mathrm{int},wall,3,7}+\\ U_{\mathrm{int},wall,5,7}A_{\mathrm{int},wall,5,7}+U_{\mathrm{int},wall,6,7}A_{\mathrm{int},wall,6,7}+\\ U_{\mathrm{int},wall,4,7}A_{\mathrm{int},wall,4,7}+U_{\mathrm{int},wall,7,adj1}A_{\mathrm{int},wall,7,adj1}+\\ U_{\mathrm{int},wall,7,adj2}A_{\mathrm{int},wall,7,adj2}+U_{\mathrm{int},wall,7,adj3}A_{\mathrm{int},wall,7,adj3}\end{array}}{\rho_{in,7}c_{in,7}V_{in,7}} \end{array}\right]$$

$$B=c_w\cdot(t_s-t_r)\cdot diag\left(\begin{array}{ccccccc}\frac{1}{\rho_{\mathrm{in},1}c_{in,1}V_{in,1}} & \frac{1}{\rho_{\mathrm{in},2}c_{in,2}V_{in,2}} & \frac{1}{\rho_{\mathrm{in},3}c_{in,3}V_{in,3}} & 0 & 0 & \frac{1}{\rho_{in,6}c_{in,6}V_{in,6}} & \frac{1}{\rho_{\mathrm{in},7}c_{in,7}V_{in,7}}\end{array}\right)$$

$$C=I_7$$

$$E_{row1}=\left[\begin{array}{ccccccc}\frac{U_{win,1}A_{win,1}+U_{roof,ext,wall,1}A_{roof,ext,wall,1}}{\rho_{in,1}c_{in,1}V_{in,1}} & \frac{\alpha_1A_{win,1}}{\rho_{in,1}c_{in,1}V_{in,1}} & \frac{U_{\mathrm{int},wall,1,adj1}A_{\mathrm{int},wall,1,adj1}}{\rho_{in,1}c_{in,1}V_{in,1}} & 0 & 0 & 0 & \frac{U_{\mathrm{int},wall,1,adj5}A_{\mathrm{int},wall,1,adj5}}{\rho_{in,1}c_{in,1}V_{in,1}} & 0\end{array}\right]$$

$$E_{row2}=\left[\begin{array}{cccccccc}\frac{U_{win,2}A_{win,2}+U_{roof,ext,wall,2}A_{roof,ext,wall,2}}{\rho_{in,2}c_{in,2}V_{in,2}} & \frac{\alpha_2A_{win,2}}{\rho_{in,2}c_{in,2}V_{in,2}} & 0 & 0 & 0 & 0 & 0 & \frac{U_{\mathrm{int},wall,2,adj6}A_{\mathrm{int},wall,2,adj6}}{\rho_{in,2}c_{in,2}V_{in,2}}\end{array}\right]$$

$$E_{row3}=\left[\begin{array}{cccccccc}\frac{U_{win,3}A_{win,3}+U_{roof,ext,wall,3}A_{roof,ext,wall,3}}{\rho_{in,3}c_{in,3}V_{in,3}} & \frac{\alpha_3A_{win,3}}{\rho_{in,3}c_{in,3}V_{in,3}} & 0 & 0 & 0 & \frac{U_{\mathrm{int},wall,3,adj4}A_{\mathrm{int},wall,3,adj4}}{\rho_{in,3}c_{in,3}V_{in,3}} & 0 & \frac{U_{\mathrm{int},wall,3,adj6}A_{\mathrm{int},wall,3,adj6}}{\rho_{in,3}c_{in,3}V_{in,3}}\end{array}\right]$$

$$E_{row4}=\left[\begin{array}{cccccccc}\frac{U_{roof,ext,wall,4}A_{roof,ext,wall,4}}{\rho_{in,4}c_{in,4}V_{in,4}} & 0 & \frac{U_{\mathrm{int},wall,4,adj1}A_{\mathrm{int},wall,4,adj1}}{\rho_{in,4}c_{in,4}V_{in,4}} & 0 & 0 & 0 & \frac{U_{\mathrm{int},wall,4,adj5}A_{\mathrm{int},wall,4,adj5}}{\rho_{in,4}c_{in,4}V_{in,4}} & 0\end{array}\right]$$

$$E_{row5}=\left[\begin{array}{cccccccc}\frac{U_{roof,ext,wall,5}A_{roof,ext,wall,5}}{\rho_{in,5}c_{in,5}V_{in,5}} & 0 & 0 & 0 & 0 & 0 & 0 & \frac{U_{\mathrm{int},wall,5,adj6}A_{\mathrm{int},wall,5,adj6}}{\rho_{in,5}c_{in,5}V_{in,5}}\end{array}\right]$$

$$E_{row6}=\left[\begin{array}{cccccccc}\frac{U_{win,6}A_{win,6}+U_{roof,ext,wall,6}A_{roof,ext,wall,6}}{\rho_{in,6}c_{in,6}V_{in,6}} & \frac{\alpha_6A_{win,6}}{\rho_{in,6}c_{in,6}V_{in,6}} & 0 & 0 & 0 & 0 & \frac{U_{\mathrm{int},wall,6,adj5}A_{\mathrm{int},wall,6,adj5}}{\rho_{in,6}c_{in,6}V_{in,6}} & 0\end{array}\right]$$

$$E_{row7}=\left[\begin{array}{cccccccc}\frac{U_{roof,7}A_{roof,7}}{\rho_{in,7}c_{in,7}V_{in,7}} & 0 & \frac{U_{\mathrm{int},wall,7,adj1}A_{\mathrm{int},wall,7,adj1}}{\rho_{in,7}c_{in,7}V_{in,7}} & \frac{U_{\mathrm{int},wall,7,adj2}A_{\mathrm{int},wall,7,adj2}}{\rho_{in,7}c_{in,7}V_{in,7}} & \frac{U_{\mathrm{int},wall,7,adj3}A_{\mathrm{int},wall,7,adj3}}{\rho_{in,7}c_{in,7}V_{in,7}} & 0 & 0 & 0\end{array}\right]$$

## References


[1] Lizana J, Chacartegui R, Barrios-Padura A, Valverde JM. Advances in thermal energy storage materials and their applications towards zero energy buildings: a critical review. Appl Energy 2017;203:219–39. https://doi.org/10.1016/j.apenergy.2017.06.008.

[2] Liu Z, Zhang X, Sun Y, Zhou Y. Advanced controls on energy reliability, flexibility and occupant-centric control for smart and energy-efficient buildings. Energy Build 2023;297:113436. https://doi.org/10.1016/j.enbuild.2023.113436.

[3] Connolly D. Heat Roadmap Europe: quantitative comparison between the electricity, heating, and cooling sectors for different European countries. Energy 2017;139:580–93. https://doi.org/10.1016/j.energy.2017.07.037.

[4] Abedrabboh K, Al-Fagih L. Applications of mechanism design in market-based demand-side management: a review. Renew Sustain Energy Rev 2023;171:113016. https://doi.org/10.1016/j.rser.2022.113016.

[5] Tang H, Wang S, Li H. Flexibility categorization, sources, capabilities and technologies for energy-flexible and grid-responsive buildings: state-of-the-art and future perspective. Energy 2021;219:119598. https://doi.org/10.1016/j.energy.2020.119598.

[6] Yin M, Cai H, Gattiglio A, Khayatian F, Smith RS, Heer P. Data-driven predictive control for demand side management: theoretical and experimental results. Appl Energy 2024;353:122101. https://doi.org/10.1016/j.apenergy.2023.122101.

[7] Wei Z, Calautit J. Predictive control of low-temperature heating system with passive thermal mass energy storage and photovoltaic system: impact of occupancy patterns and climate change. Energy 2023;269:126791. https://doi.org/10.1016/j.energy.2023.126791.

[8] Amato V, Knudsen MD, Petersen S. Dual-zone economic model predictive control of residential space heating for demand response using a single heat meter. Energy Build 2023;281:112759. https://doi.org/10.1016/j.enbuild.2022.112759.

[9] Kaspar K, Ouf M, Eicker U. A critical review of control schemes for demand-side energy management of building clusters. Energy Build 2022;257:111731. https://doi.org/10.1016/j.enbuild.2021.111731.

[10] Guelpa E, Verda V. Demand response and other demand side management techniques for district heating: a review. Energy 2021;219:119440. https://doi.org/10.1016/j.energy.2020.119440.

[11] Hua P, Wang H, Xie Z, Lahdelma R. District heating load patterns and short-term forecasting for buildings and city level. Energy 2024;289:129866. https://doi.org/10.1016/j.energy.2023.129866.

[12] Li H, Sun Q, Zhang Q, Wallin F. A review of the pricing mechanisms for district heating systems. Renew Sustain Energy Rev 2015;42:56–65. https://doi.org/10.1016/j.rser.2014.10.003.
[13] Song J, Wallin F, Li H. District heating cost fluctuation caused by price model shift. Appl Energy 2017;194:715–24. https://doi.org/10.1016/j.apenergy.2016.09.073.
[14] Dominković DF, Wahlroos M, Syri S, Pedersen AS. Influence of different technologies on dynamic pricing in district heating systems: comparative case studies. Energy 2018;153:136–48. https://doi.org/10.1016/j.energy.2018.04.028.
[15] Zhang J, Ge B, Xu H. An equivalent marginal cost-pricing model for the district heating market. Energy Pol 2013;63:1224–32. https://doi.org/10.1016/j.enpol.2013.09.017.
[16] Helen company official website. 2023. https://www.helen.fi/en/heating/district-heating/district-heat-prices. [Accessed 13 December 2023].
[17] Åberg M, Fälting L, Forssell A. Is Swedish district heating operating on an integrated market? - differences in pricing, price convergence, and marketing strategy between public and private district heating companies. Energy Pol 2016;90:222–32. https://doi.org/10.1016/j.enpol.2015.12.030.
[18] Yuan X, Heikari L, Hirvonen J, Liang Y, Virtanen M, Kosonen R, et al. System modelling and optimization of a low temperature local hybrid energy system based on solar energy for a residential district. Energy Convers Manag 2022;267:115918. https://doi.org/10.1016/j.enconman.2022.115918.
[19] Bloess A, Schill WP, Zerrahn A. Power-to-heat for renewable energy integration: a review of technologies, modeling approaches, and flexibility potentials. Appl Energy 2018;212:1611–26. https://doi.org/10.1016/j.apenergy.2017.12.073.
[20] Wilczynski EJ, Chambers J, Patel MK, Worrell E, Pezzutto S. Assessment of the thermal energy flexibility of residential buildings with heat pumps under various electric tariff designs. Energy Build 2023;294:113257. https://doi.org/10.1016/j.enbuild.2023.113257.
[21] Li Y, Cui Y, Song Z, Zhao X, Li J, Shen C. Eco-economic performance and application potential of a novel dual-source heat pump heating system. Energy 2023;283:128478. https://doi.org/10.1016/j.energy.2023.128478.
[22] Huang S, Yu H, Zhang M, Qu H, Wang L, Zhang C, et al. Advances, challenges and outlooks in frost-free air-source heat pumps: a comprehensive review from materials, components to systems. Appl Therm Eng 2023;234:121163. https://doi.org/10.1016/j.applthermaleng.2023.121163.
[23] Chesser M, Lyons P, O'Reilly P, Carroll P. Air source heat pump in-situ performance. Energy Build 2021;251. https://doi.org/10.1016/j.enbuild.2021.111365.
[24] Sezen K, Gungor A. Performance analysis of air source heat pump according to outside temperature and relative humidity with mathematical modeling. Energy Convers Manag 2022;263:115702. https://doi.org/10.1016/j.enconman.2022.115702.
[25] Alghamdi SM, Ajour MN, Abu-Hamdeh NH, Karimipour A. Using PCM for building energy management to postpone the electricity demand peak load and approving a new PID controller to activate alternative chiller. J Build Eng 2022;57:104884. https://doi.org/10.1016/j.jobe.2022.104884.
[26] Zhao BY, Zhao ZG, Li Y, Wang RZ, Taylor RA. An adaptive PID control method to improve the power tracking performance of solar photovoltaic air-conditioning systems. Renew Sustain Energy Rev 2019;113. https://doi.org/10.1016/j.rser.2019.109250.
[27] Li W, Zhang J, Zhao T, Ren J. Experimental study of an indoor temperature fuzzy control method for thermal comfort and energy saving using wristband device. Build Environ 2021;187:107432. https://doi.org/10.1016/j.buildenv.2020.107432.
[28] Li X, Zhang C, Zhao T, Han Z. Adaptive predictive control method for improving control stability of air-conditioning terminal in public buildings. Energy Build 2021;249:111261. https://doi.org/10.1016/j.enbuild.2021.111261.
[29] Wu Z, Mu Y, Deng S, Wang J, Bai Y, Xue J, et al. Towards comfortable and cost-effective indoor temperature management in smart homes: a deep reinforcement learning method combined with future information. Energy Build 2022;275:112491. https://doi.org/10.1016/j.enbuild.2022.112491.
[30] Peng Y, Lei Y, Tekler ZD, Antanuri N, Lau SK, Chong A. Hybrid system controls of natural ventilation and HVAC in mixed-mode buildings: a comprehensive review. Energy Build 2022;276:112509. https://doi.org/10.1016/j.enbuild.2022.112509.
[31] Shaikh PH, Nor NBM, Nallagownden P, Elamvazuthi I, Ibrahim T. A review on optimized control systems for building energy and comfort management of smart sustainable buildings. Renew Sustain Energy Rev 2014;34:409–29. https://doi.org/10.1016/j.rser.2014.03.027.
[32] Lind J, Möllerström E, Averfalk H, Ottermo F. Energy flexibility using the thermal mass of residential buildings. Energy Build 2023;301. https://doi.org/10.1016/j.enbuild.2023.113698.
[33] Foteinaki K, Li R, Péan T, Rode C, Salom J. Evaluation of energy flexibility of low-energy residential buildings connected to district heating. Energy Build 2020;213:109804. https://doi.org/10.1016/j.enbuild.2020.109804.
[34] Hu M, Xiao F, Wang L. Investigation of demand response potentials of residential air conditioners in smart grids using grey-box room thermal model. Appl Energy 2017;207:324–35. https://doi.org/10.1016/j.apenergy.2017.05.099.
[35] Hu M, Xiao F. Price-responsive model-based optimal demand response control of inverter air conditioners using genetic algorithm. Appl Energy 2018;219:151–64. https://doi.org/10.1016/j.apenergy.2018.03.036.
[36] Salo S, Jokisalo J, Syri S, Kosonen R. Individual temperature control on demand response in a district heated office building in Finland. Energy 2019;180:946–54. https://doi.org/10.1016/j.energy.2019.05.035.
[37] Romanchenko D, Nyholm E, Odenberger M, Johnsson F. Impacts of demand response from buildings and centralized thermal energy storage on district heating systems. Sustain Cities Soc 2021;64:102510. https://doi.org/10.1016/j.scs.2020.102510.
[38] Yuan X, Lindroos L, Jokisalo J, Kosonen R, Pan Y, Jin H. Demand response potential of district heating in a swimming hall in Finland. Energy Build 2021;248:111149. https://doi.org/10.1016/j.enbuild.2021.111149.
[39] Du Y, Zhou Z, Zhao J. Multi-regional building energy efficiency intelligent regulation strategy based on multi-objective optimization and model predictive control. J Clean Prod 2022;349:131264. https://doi.org/10.1016/j.jclepro.2022.131264.
[40] Xiong C, Sun Z, Meng Q, Li Z, Wei Y, Zhao F, et al. A simplified improved transactive control of air-conditioning demand response for determining room set-point temperature: experimental studies. Appl Energy 2022;323:119521. https://doi.org/10.1016/j.apenergy.2022.119521.
[41] Li Z, Sun Z, Meng Q, Wang Y, Li Y. Reinforcement learning of room temperature set-point of thermal storage air-conditioning system with demand response. Energy Build 2022;259:111903. https://doi.org/10.1016/j.enbuild.2022.111903.
[42] Li Z, Meng Q, Wei Y, Zhang L, Sun Z, Lei Y, et al. Dynamic room temperature setpoints of air-conditioning demand response based on heat balance equations with thermal comfort model as constraint: on-site experiment and simulation. J Build Eng 2023;65:105798. https://doi.org/10.1016/j.jobe.2022.105798.
[43] Mamdani EH. Application of fuzzy algorithms for control of simple dynamic plant. Proc Inst Electr Eng 1974;121:1585–8. https://doi.org/10.1049/PIEE.1974.0328.
[44] Hua P, Wang H, Xie Z, Lahdelma R. Multi-criteria evaluation of novel multi-objective model predictive control method for indoor thermal comfort. Energy 2024;289:129883. https://doi.org/10.1016/j.energy.2023.129883.
[45] NORD POOL official website. 2023. https://www.nordpoolgroup.com/. [Accessed 13 December 2023].
[46] Savolainen R, Lahdelma R. Optimization of renewable energy for buildings with energy storages and 15-minute power balance. Energy 2022;243:123046. https://doi.org/10.1016/j.energy.2021.123046.
[47] Rikkas R, Lahdelma R. Energy supply and storage optimization for mixed-type buildings. Energy 2021;231:120839. https://doi.org/10.1016/j.energy.2021.120839.